The Dissertation Committee for Sucharit Katyal Certifies that this is the approved version of the following dissertation:

Measuring visual stimulation and attention signals in human superior colliculus using high-resolution fMRI

Committee:

David Ress, Supervisor

Lawrence Cormack, Co-Supervisor

Alexander Huk

Michael Beauchamp

Mary Hayhoe

Measuring visual stimulation and attention signals in human superior colliculus using high-resolution fMRI

by

Sucharit Katyal, B.E.; M.Sc.

Dissertation

Presented to the Faculty of the Graduate School of

The University of Texas at Austin

in Partial Fulfillment

of the Requirements

for the Degree of

Doctor of Philosophy

The University of Texas at Austin

May 2013

Dedication

According to the philosophy of science of Yoga, the quest for Truth is the inherent longing of an individual's mind. The word 'consciousness' in Sanskrit language is known by the terms *Purusa* or *Shiva* and is synonymous with such a Truth. What humans through self-reflection refer to as subjectivity or consciousness is actually omnipresent, though most clearly reflected by the human mind. Therefore, instead of consciousness being a generative property of the human mind, and therefore the brain, mind itself is a step through the process of evolution. In fact, the process of evolution is the process of evolution of consciousness. In successive stages of this evolution, consciousness goes on a journey from crude to subtle, starting in the material realm, followed by the mental or psychic realm and culminating in the spiritual realm. According this philosophy, the mind-body "problem" does not exist for dualism is only an apparent sage of an individual's mind. The unveiling of this seeming illusion begins by understanding the continuity of the physico-psychic-spirirual parallelism, though proceeds only through means of spiritual practices or *sadhana*. S*adhana* should not be identified with religion or religiosity and in the beginning is best approached with full skepticism, for at its core lies the non-acceptance of dogma of any kind. It may, however, seem psychologically daunting in the beginning, because it is a process of purification of the mind, but becomes easier as one slowly gets established in a universal ideation for a substantial part of their waking life. The final goal of *sadhana* then is the realization of this inherent non-duality of the physico-psychic-spiritual realms, which in mystical terms is often known as 'realization' or 'liberation'.

I fully and completely dedicate myself to understanding of the Truth in its purest form not mired by dogma of any kind, and for that I take the path of science and more importantly the science of mind in addition to my spiritual path. I dedicate this

dissertation and the quest of my doctoral years, to the individual I identify as my spiritual preceptor, my Gurudeva, whom I love most dearly, Shrii Shrii Anandamurtii*ji*.

Acknowledgements

Measuring visual stimulation and attention signals in human superior colliculus using high-resolution fMRI

Sucharit Katyal, Ph.D.

The University of Texas at Austin, 2013

Supervisor: David Ress

The superior colliculus (SC) is a laminated oculomotor structure in the midbrain. In non-human primates SC has long been known to contain a retinotopically-organized map of visual stimulation in its superficial layers, which is aligned to a map of saccadic eye movements in the deeper layers. Microstimulation and electrophysiology experiments have shown that SC also plays a key role in covert visuospatial attention and suggest that attentional modulation also occurs in a retinotopic manner. Retinotopic organization of the visual field can be non-invasively mapped in humans using functional MRI with a technique called phase-encoded retinotopy. In this technique, rotating wedges and expanding rings of visual stimuli are used to map the polar angle and eccentricity dimensions of a polar coordinates system, respectively. A similar technique can also be used to map spatial attention by keeping the visual stimulus constant and cueing subjects to attend to apertures of rotating wedges and expanding rings within the stimulus. A previous study using fMRI has shown the polar angle representation of visual stimulation in human SC but was unable to find a representation of eccentricity. This work uses high-resolution fMRI along with special surface analysis techniques developed in our lab to demonstrate maps of both polar angle and eccentricity for visual stimulation. Moreover, visual attention is also shown to be topographically organized within SC and in

registration with visual stimulation. Finally, in human visual cortex, fMRI is known to show activity for sustained spatial attention even in the absence of a significant visual stimulus, an attentional "base response". In this work, SC is shown to exhibit a similar sustained attention base response using a threshold-contrast detection paradigm. This base response was compared with a response for attention with visual stimulation. The peak amplitude of the base response occurred more deeply within SC tissue than the peak for attention with stimulation. It is proposed that this reflects the specific attentional enhancement of the deeper visuomotor neurons, which are hypothesized to be a direct neuronal correlate of the oculomotor theory of attention.

Table of Contents

List of Tables

List of Figures

Chapter I: Introduction

The term colliculus comes from Latin for "hill" and refers to two pairs (left and right) of nuclei located at the dorsal surface of the midbrain in the brainstem. The more rostral of the pairs is known as the superior colliculus (SC). Evolutionarily, SC is the same structure that in non-mammals is known as the optic tectum. Throughout its evolutionary history, from the optic tectum to SC, this region has been involved in transforming sensory signals into motor commands relevant to orienting behavior (Stein et al., 2002). In primates, the SC sensorimotor functionality is focused primarily upon the visual modality. SC receives information from visual as well as other sensory modalities, and translates them into orientation of gaze (eye and head movements). In addition to such overt shifts of orientation, primate SC has also been implicated in covert shifts of attention. Academic literature on the anatomical organization of the SC, its response to visual stimulation and its role in attention is reviewed here.

STRUCTURAL AND FUNCTIONAL ORGANIZATION OF PRIMATE SC

SC is a laminar structure consisting of seven alternating layers of cell bodies and fibers. The outer three layers, *stratum zonale*, *stratum griseum superficiale*, and *stratum opticum* are together called the superficial layers. The next two layers, *stratum griseum intermediale*, and *stratum album intermediale*, form the intermediate layers, and finally *stratum griseum profundum* and *stratum album profundum* are the deep layers. By virtue of anatomical and functional similarities, the intermediate and deep layers are together also known simply as the deeper layers. It has long been known that there is a distinct functional division between superficial and deeper layers of the SC. The superficial layers are involved in processing visual signals while deeper layers gather signals from multiple sensory modalities and combine the sensory signals to generate oculomotor

signals (Mays and Sparks, 1980; Wurtz and Albano, 1980). There is also a cascade of interlaminar connections that project from superficial to deeper layers (May, 2006; Mooney et al., 1988; Moschovakis et al., 1988).

Superficial layers

The superficial layers of SC primarily contain visually responsive neurons, with heavy projections directly from the retina (Leventhal et al., 1981; Perry and Cowey, 1984; Pollack and Hickey, 1979). In addition, superficial layers also receive afferents from striate and extrastriate cortical areas (Finlay et al., 1978; Fries, 1984; Fries and Distel, 1983; Lui et al., 1995). Outputs from superficial layers are primarily ascending and include projections to the inferior and lateral pulvinar (Benevento and Standage, 1983), and dorsal and ventral lateral geniculate nuclei in the thalamus (Harting et al., 1980; May, 2006; Wilson et al., 1995) among other regions.

Early electrophysiology studies in non-human primates showed that there is a retinotopic organization of visual stimulation signals in the superficial layers (Cynader and Berman, 1972; Goldberg and Wurtz, 1972a). Each colliculus responds to the contralateral hemifield. Specifically, polar angle is represented along the medial-lateral direction, with neurons having receptive fields in the upper visual field located medially and those having receptive fields in the lower visual field located laterally. Eccentricity is represented along the rostral-caudal direction, with foveal eccentricities located in the rostral and peripheral eccentricities located in the caudal part of SC. There is a slight angular tilt in the map such that the rostral portion of the map is shifted towards the lateral side and caudal portion towards the medial side. Along the eccentricity dimension, the representation of near foveal eccentricities is magnified, such that, the inner 10° of visual angle take up over a third of the colliculus and receptive field sizes of neurons

increase with increasing eccentricities (Cynader and Berman, 1972). Within the superficial layers, the receptive field sizes of the visual neurons increase with depth (Cynader and Berman, 1972; Goldberg and Wurtz, 1972a; Tiao and Blakemore, 1976).

Deeper layers

The deeper layers contain oculomotor neurons that discharge prior to saccadic eye-movements as well as unisensory and multisensory neurons for visual, auditory and somatosensory modalities. The deeper layers receive afferents from multiple sensory and association areas in the cortex including frontal eye fields (FEF) (Fries, 1984; Komatsu and Suzuki, 1985; Kunzle et al., 1976; Sommer and Wurtz, 2000), premotor, prefrontal (Fries, 1984; Goldman and Nauta, 1976), extrastriate (Lui et al., 1995), posterior parietal (Fries, 1984; Lynch et al., 1985), auditory association, somatosensory association (Fries, 1984; Harting et al., 1992; Wallace et al., 1993) cortices (May, 2006; Sparks and Hartswich-Young, 1989). They also have reciprocal connections with a host of brainstem nuclei (Edwards et al., 1979; Meredith et al., 1991) that are responsible for generating saccadic eye and head movements. Deeper layers also send ascending projections to thalamic nuclei, including the lateral geniculate nucleus (LGN), the medial dorsal nucleus, several intralaminar nuclei (May, 2006).

Aligned with the visual stimulation map in the superficial layers is a map of saccadic eye-movements in the intermediate layers (Robinson, 1972; Schiller and Stryker, 1972; Sparks and Nelson, 1987). Here, saccades of stereotypical amplitudes and direction can be evoked by microstimulation (small current injections) at spatially precise locations within the SC map (Schiller and Koerner, 1971; Wurtz and Goldberg, 1972). Specifically, there is not a one-to-one mapping from neurons to precise saccade vectors but rather each neuron has a spatially tuned movement field (Wurtz and Goldberg, 1972)

and the final position of the saccades is determined by a population-averaged response of a large number of oculomotor neurons (Lee et al., 1988). Similar to the visual responses, the size of the movement fields also increases with increasing eccentricity on the map. Near-foveal movement fields are smaller in size (~5°) and have steeper gradients while those farther from the fovea are larger (20—30°) with more gradual response gradients (Sparks et al., 1976).

Based on their activity profiles prior to saccade onset, the oculomotor neurons of the intermediate layers are divided into three types: buildup, burst and fixation (Munoz and Wurtz, 1993; Munoz and Wurtz, 1995a; Wurtz and Goldberg, 1972). Buildup neurons start firing after a short delay following cue onset and persist with a low frequency discharge. At ~100 ms before the saccade buildup neurons have a gradual increase in activity, reflecting a saccade preparatory response, followed by a high-frequency discharge starting ~25 ms before saccade onset. The burst neurons, on the other hand, have a brief cue onset response and then remain largely silent before firing a high-frequency discharge upon saccade onset. Finally, the fixation neurons are located near the rostral pole of SC and respond specifically when the monkey is fixating actively (Munoz and Wurtz, 1993). Fixation neurons gradually reduce their response as the buildup neurons increase their activity and, finally, become silent at the onset of burst activity (Munoz and Wurtz, 1995b). The fixation neurons when active also have the property of sending inhibitory signals to the saccade-related buildup and burst neurons in the caudal portions of SC.

The deeper layers of SC also contain a map of other sensory modalities including somatosensory and auditory in retinal coordinates, which is aligned to the visual map (Drager and Hubel, 1975; Groh and Sparks, 1996; Jay and Sparks, 1987; Wallace et al., 1993). Therefore, across the SC, sensory and motor organization of neurons is such that,

within a depth column, neurons correspond to roughly the same retinal coordinates (Meredith et al., 1992). This mapping scheme emphasizes the role of SC as a sensory signal to gaze transformation center.

ROLE OF SC IN VISUAL ATTENTION

While electrical microstimulation in SC intermediate layers has long been known to evoke saccadic eye movements, recent studies have shown that intermediate layer microstimulation below the saccadic threshold, i.e., at current values for which saccades are not evoked, improves monkeys' behavioral performance akin to attentional improvement, also in a retinotopic manner. In one study, performance thresholds for motion discrimination in monkeys were significantly improved upon subthreshold microstimulation at the site corresponding to the stimulus (Muller et al., 2005). While, another study demonstrated that subthreshold microstimulation enhanced monkeys' ability to perform a change-blindness task, specifically when the stimulation was applied to the location where the upcoming trial would have a change in the stimulus (Cavanaugh et al., 2006; Cavanaugh and Wurtz, 2004). Similar effects for modulation of attention by subthreshold microstimulation have also been shown in monkey cortical region FEF (Moore and Fallah, 2004). Conversely, cue-evoked attention has also been shown to modulate saccade trajectories evoked by SC microstimulation. Kustov and Robinson (Kustov and Robinson, 1996) showed that saccades evoked by microstimulation in the SC were systematically shifted towards the left or right, if preceded by an exogenous cue at a location left or right of the saccade target respectively. This influence of exogenously cued attention on the population-averaging scheme that determines the saccade vector was indicative of attentional signals being encoded in oculomotor coordinates. All together, these results together indicate a tight link between overt saccadic control and

covert cue-evoked attention in SC. Such an overlap of overt and covert processing in the brain is consistent with a *premotor* or *oculomotor theory* of spatial attention (Moore et al., 2003; Rizzolatti et al., 1987; Rizzolatti et al., 1994). According to the oculomotor theory, the initial programming for the preparation of both overt and covert orientation takes place within common neural substrates, with the overt movement behavior a serially added step to this initial preparation process. Based on human psychophysics in the past few decades there has been some disagreement over the relationship between overt and covert orientation (see next section for alternate hypotheses). However, more recent studies have provided direct neural evidence for an overlap between brain regions that mediate eye movements and attention in support of an oculomotor theory. Moreover, the evidence for a subcortical nucleus such as the SC as a putative effector in this process is even more recent.

At the level of single-unit electrophysiology, early work in macaques had shown that the response of superficial layer visual neurons was enhanced if the location of the visual stimulus was also the target for an upcoming saccade (Goldberg and Wurtz, 1972b; Wurtz and Mohler, 1976). However, since in those experiments the visual stimulus spatially coincided with the saccade target, it was unclear if the neuronal enhancement was simply a planned saccade, or it would also occur for covert attention without an ensuing saccade. Strictly speaking within the framework of the oculomotor theory of attention, it would not be possible to covertly attend in the absence of planning an eye movement (Hoffman and Subramaniam, 1995; Moore et al., 2003; Shepherd et al., 1986). Nonetheless, it is known, at least in human primates, that spatial attention can be split over separate noncontiguous spatial locations (Awh and Pashler, 2000; Kramer and Hahn, 1995; McMains and Somers, 2004), implying that attention may be covertly applied to one region of space while planning to make an eye movement at another one.

This question of attentional modulation vs. saccadic planning in SC neurons was addressed in a more recent study designed to dissociate the spatial locus of attention from the target of eye movements (Ignashchenkova et al., 2004). In their paradigm monkeys were peripherally cued to covertly attend to one of two diametrically opposite spatial locations. Followed by a short delay, a stimulus appeared at the cued location indicating the monkeys to make a saccade to one of two targets placed orthogonally to the cue. Based on single-unit response properties, the authors distinguished between three classes of neuronal subtypes within SC, the superficial-layer visual neurons, and intermediate-layer visuomotor and motor neurons. Both the visual neurons, which respond to visual stimulation, and visuomotor neurons, which respond to visual stimulation as well as fire before saccades, had an enhancement of response by the cue for the stimulus; whereas, only the visuomotor neurons had a baseline response during the delay period between the cue and stimulus. Finally, the motor neurons, which only fire for saccades, did not have any cue-evoked enhancement. Additionally, it was noted that the attentional modulation of the visuomotor neurons occurred specifically for peripheral and not central cues, suggesting that attention signals in the SC may be purely exogenous in nature. This delay period baseline enhancement of visuomotor neurons was proposed to be a direct correlate of the oculomotor theory of attention.

Recent work by Krauzlis and colleagues (Lovejoy and Krauzlis, 2009; Zenon and Krauzlis, 2012) using reversible deactivations of the colliculus to demonstrate attentional neglect in monkeys has indicated that SC may actually be a critical component of the attention network. Monkeys were cued to attend to one of four diagonal locations where random dot stimuli would be shown (Lovejoy and Krauzlis, 2009). Monkeys' task was to detect the direction of a brief coherent motion signal at the cued location, while ignoring another coherent motion signal in a different direction at the diagonally opposite

distractor location. It was observed that when a muscimol (GABA agonist) injection was applied to inhibit the intermediate and deep layers of SC corresponding to the retinotopic location of the cue, monkeys were not able to maintain attention at the cued location and reported the motion direction of the distractor. The performance of the monkeys was unimpaired when there was no coherent motion at the distractor location indicating that the impairment was not visual in nature. This deficit is analogous to the well-known spatial attentional neglect syndrome in humans (Rafal, 1994), where patients with brain damage tend to ignore certain regions of space while still being able to perform visual sensory tasks in those regions. Subsequently, the group showed that this behavioral deficit in monkeys occurs without a concomitant change in the modulation of the motion processing areas of visual cortex by the task (Zenon and Krauzlis, 2012). This suggests that SC may not project its attention related signals posteriorly to early visual cortex, while still being responsible for influencing behavior, thereby, making its role in attention even more critical.

Neuropsychological evidence for attention in human SC

Evidence from neuropsychology in patients with focal damage to the SC is generally rare, as midbrain lesions often incur a high mortality rate, marked motor deficits and/or considerable cortical damage (Weddell, 2004). However, there are instances of SC damage in progressive supranuclear palsy and strokes that have been occasionally investigated and have shown deficits in deployment of attention (Posner and Petersen, 1989; Rafal et al., 1988). Studies with such patients have implicated an important role for the SC, especially in the phenomenon of "inhibition of return" (IOR) (Posner et al., 1985; Sapir et al., 1999). According to IOR, after deploying attention to a particular location in space, once attention is withdrawn from that location, subjects tend

to be slower to redeploy attention at the same location. Unit electrophysiology studies in monkeys (Bell et al., 2004; Fecteau et al., 2004) and fMRI studies in humans (Anderson and Rees, 2011) have also confirmed the role of SC in IOR. Additionally, the phenomenon of attentional neglect, which is typically observed patients with frontal and parietal damage (Rafal, 1994), has also been observed in a rare patient with focal damage to the SC (Weddell, 2004). As mentioned in the previous section, this is corroborated by the SC inactivation studies in monkeys (Lovejoy and Krauzlis, 2009).

PSYCHOPHYSICS AND NEUROIMAGING IN HUMANS

An oculomotor theory of attention

There has been a long history of relating overt eye movements/motor programming to covert visual spatial attention (Ferrier, 1890; von Helmholtz, 1866/1962); for review see (Moore et al., 2003). However, human psychophysics experiments over the past few decades have provided conflicting results regarding the relationship between the neural code for programming of overt and covert shifts of orientation (Hoffman and Subramaniam, 1995; Klein, 1980; Posner, 1980; Rizzolatti et al., 1987; Shepherd et al., 1986), suggesting the possibility of three hypotheses regarding relationship of their neural substrates (Corbetta, 1998; Shepherd et al., 1986): 1) the independence hypothesis, according to which the two processes occur separately in the brain, 2) the interdependence hypothesis, suggesting some amount of overlap and separation in their computation, and, 3) the identity hypothesis, whereby programming for eye movements and visual attention is essentially the same neural code. The identity hypothesis is also commonly known as the visuomotor or oculomotor hypothesis of attention (Moore et al., 2003; Rizzolatti et al., 1987). Some work in support of

oculomotor origins of attention in non-human primate particularly within SC has been outlined above.

In human cerebral cortex, functional magnetic resonance imaging (fMRI) has been used to compare the neural correlates of overt and covert shifts of attention. Multiple studies have yielded similar results showing that the two largely overlap at the level of cortex, repeatedly showing a fronto-parietal network of activation for both overt and covert attention (Beauchamp et al., 2001; Corbetta, 1998; de Haan et al., 2008; Nobre et al., 2000; Perry and Zeki, 2000). This network includes FEF, intraparietal sulcus, lateral occipital sulcus and medial occipital gyrus, among other areas. These studies largely support an oculomotor theory for the origin of attention, although, at least one study also interprets these results from the point of the interdependence hypothesis (Corbetta, 1998). Studies that have controlled for task-related affects between overt and covert shifts (Beauchamp et al., 2001; de Haan et al., 2008) show that overt eye movements evoke greater activation within these regions than covert shifts of attention, which would be expected if covert attention and eye movements shared a common basic network, with overt movements requiring extra processing as predicted by the oculomotor theory.

FMRI of SC

Despite the large body of research available on the SC in non-human primates and other mammals, there have been relatively few studies of SC in humans using fMRI. This has to with the methodological challenges associated with its imaging, such as small size and proximity to large blood vessels that are known to produce pulsatile physiologic noise (Wall et al., 2009). Though, there has been some reported work suggesting

techniques for overcoming some of these methodological challenges (Glover et al., 2000; Wall et al., 2009).

Despite these challenges, some early studies investigating oculomotor and attention related signals in whole brain fMRI did show functional signals in the SC. SC was shown to be active for attention to motion (Buchel et al., 1998), have lateralized signals for visual stimulation (DuBois and Cohen, 2000), contain a representation for eye, head and gaze movements (Petit and Beauchamp, 2003), and be involved in visual search (Gitelman et al., 2002). Recent imaging studies of the SC that have probed it using more localized slice prescriptions and with higher-spatial resolution, have confirmed the contralateral representation of saccades in SC (Krebs et al.), shown saccade-related activity in multiple brainstem oculomotor regions including SC (Linzenbold et al., 2011), and also shown reach-related upper limb signals in the superficial and deep SC (Linzenbold and Himmelbach, 2012).

The retinotopic organization of visual stimulation signals in the SC has been probed using phase-encoded retinotopic techniques (DeYoe et al., 1994; DeYoe et al., 1996; Engel et al., 1997; Sereno et al., 1995). Schneider and Kastner (Schneider and Kastner, 2005, 2009) showed that polar angle representation of the visual field was retinotopically organized within SC, similar to the monkey maps (Cynader and Berman, 1972). However, despite attempts, they were not able to show a retinotopic progression for eccentricity (Schneider and Kastner, 2005).

Attention related modulation of SC has also been observed using fMRI (Buchel et al., 1998; Schneider and Kastner, 2009). Schneider and Kastner (Schneider and Kastner, 2009) showed the presence of sustained spatial attention signals within SC, which were stronger than those measured in human LGN. However, the question of spatial specificity of attentional modulation in SC has not yet been addressed.

Behavioral control of visual attention

Since neural responses within SC are known to be modulated by attention (Buchel et al., 1998; Ignashchenkova et al., 2004; Schneider and Kastner, 2009; Wurtz and Mohler, 1976), it is important that, while performing fMRI measurements, the cognitive state of the subjects be controlled by having them perform an attentionally demanding behavioral task over the course of the experiment (Huk et al., 2001). Such behavioral control would potentially, 1) keep the subjects' mind from wandering during the course of the session and therefore adding "cognitive noise" to the data, as well as, 2) enhance the BOLD signal levels, which could enable better detection of the visual stimulation related responses within the midbrain tissue.

The behavior of subjects in visual detection and discrimination tasks can be controlled over the course of the experimental session by using the psychophysics technique of an *N*-up-1-down staircase (Garcia-Perez, 1998) to regulate the difficulty of an attentionally demanding task. In such a staircase procedure stimulus thresholds are adapted over the course of a session by making the task more difficult after *N* correct trials and easier after a single incorrect trial, in a stepwise manner. Using this technique, as the subjects' state of arousal waxes and wanes during the course of an experimental session, the task difficulty adjusts to maintain a consistent level of performance.

GOALS OF THIS DISSERTATION

This dissertation will attempt to answer some questions about the organization of visual stimulation and attention signals in human SC using high-resolution fMRI as well as demonstrate the use of some novel methodological procedures for the analysis of high-resolution data in human midbrain (Katyal et al., 2012).

In my first set of experiments (Chapter III), I try to replicate the retinotopic organization of visual stimulation in SC along polar angle using a higher spatial

resolution than the previous studies (Katyal et al., 2010; Schneider and Kastner, 2005, 2009). Evidence from non-human primate research shows that attentional response of SC is also topographically organized. I test if there is a retinotopic organization of visual attention signals along polar angle as well and if so, whether the attention signals are spatially in register with visual stimulation. Anatomical data suggest that in addition to the superficial layers, visually responsive neurons (either unimodal or multimodal) are also present the deep layers of SC (Wallace et al., 1996). Attentional modulation of responses, however, has been only observed within the superficial and intermediate layer neurons (Goldberg and Wurtz, 1972b; Ignashchenkova et al., 2004; Wurtz and Mohler, 1976). Using novel surface-based techniques developed in our lab (Khan et al., 2011; Ress et al., 2007), I also characterize the fMRI response for visual stimulation and attention within the depth of SC.

In the second set of experiments (Chapter IV), I investigate if visual stimulation signals are also retinotopically organized along the eccentricity dimension. As described before, previous attempts to measure the retinotopic organization along eccentricity in SC have not been successful. The putative reasons for this and their implication on making such measurements in SC are also discussed. I also test if visual attention signals are topographically organized along the eccentricity dimension.

In the third and final set of experiments (Chapter V), I investigate the nature of different types of attention signals in human SC. Previous fMRI studies have shown modulation of SC activity while attending to visual stimuli, which by themselves evoke a visual response in SC (Buchel et al., 1998; Schneider and Kastner, 2009). Here, I investigate if SC also has a response for attention in the absence of significant visual stimulation, an attentional *base response*. Such a response has been previously observed using fMRI in visual cortical areas (Kastner et al., 1999; Ress et al., 2000; Silver et al.,

2007). Having measured an attentional response in SC toward a high-contrast stimulus in Chapter III, I present a comparison of the two responses with respect to their depth in SC. As described in the previous sections, studies in monkeys have shown that attention enhances the response of both superficial layer visual neurons and intermediate layer visuomotor neurons, of which the latter are suggested to be a correlate of the oculomotor theory of attention. Extending this, I hypothesize that if a base response were present in the SC, due to non-stimulation of the superficial layer visual neurons, it would occur deeper in the tissue than the attentional response to a high-contrast stimulus.

Chapter II: General methods

This chapter describes the methods common for the experiments reported in this dissertation.

SUBJECTS

Informed consent was obtained from all subjects based on a protocol approved by the University of Texas at Austin's Institutional Review Board. All subjects had normal or corrected-to-normal visual acuity.

VISUAL DISPLAYS AND STIMULUS PROTOCOLS

All visual stimuli were generated using MATLAB (MathWorks, Natick, MA) running PsychToolbox-3 (Brainard, 1997; Pelli, 1997) on a Macintosh Pro computer. There were two display devices that were used in these experiments: 1) An LCD projector, which displayed the stimulus onto a back-projection screen mounted inside the scanner bore 0.49 m from the subject's eyes, and 2) a 43-inch LCD television, placed behind the scanner bore and viewed through a mirror placed upon the head-coil 2.8 m from the subject's eyes. Both displays were calibrated for gamma variations. Because display #2 had been modified for use near a MRI scanner, its screen backlight illumination was somewhat non-uniform, and exhibited bands of luminance variations across the screen. These luminance variations were measured and corrected before presenting the stimuli to ensure a spatial flat field. In order to correct these luminance variations, a photograph was taken of the screen with a camera capable of capturing raw images. Because the camera itself had spatial inhomogeneity in capturing luminance, due to aberrations of the camera optics, another photograph was taken of a clear sky at dusk, which served as an isoluminant control image. This control image was then fit with a 2D quadratic polynomial surface to get rid of the high-frequency noise in the image not

attributed to the aberrations of the camera optics. The fit explained ~95% of the variance. The original image of the screen was then normalized by this fit surface to give a mask. Finally this mask was subtracted from the background gray image rendered onto the screen giving a spatially flat-fielded display.

Display #1 had a wider field of view (approximately 20° × 31°), as compared to the second (approximately 14° × 23°) and was therefore used in both the retinotopy experiments. However, the back-projection screen for display #1 had a strong scattered-light component, and thereby a poorer contrast response. So, for the base response contrast-detection experiments the display #2 was used.

Phase-encoded retinotopic mapping

Topographic organization of the visual field can be non-invasively mapped using a well-known functional imaging approach called phase-encoded retinotopy (DeYoe et al., 1994; DeYoe et al., 1996; Engel et al., 1997; Sereno et al., 1995). In this technique, rotating wedges and expanding rings of visual stimuli are used to map the polar angle and eccentricity dimensions of a polar coordinates system, respectively. As the stimulus periodically moves across the visual field it creates a travelling wave of activity across topographically organized visual brain regions. The time-series data at each spatial sampling point (in fMRI, a voxel) is fit with a sinusoid at the stimulus repetition frequency, a procedure known as coherence analysis. This procedure provides a magnitude, coherence and phase value at each voxel. The coherence value is equivalent to the correlation coefficient of the time-series with its best-fit sinusoid and the phase of a voxel corresponds to its location in the visual field.

A similar phase-encoded technique can also be used to map visual spatial attention by keeping the stimulus field constant throughout the experiment and cueing subjects to attend to apertures of rotating wedges or expanding rings within the visual stimulus in a periodic manner (Brefczynski and DeYoe, 1999).

These retinotopic techniques have traditionally used contrast-reversing checkerboards as visual stimuli. However, unlike early visual cortical areas that respond strongly to luminance contrast, SC visual neurons have a weaker contrast response (Cynader and Berman, 1972; Schneider and Kastner, 2005). Instead, SC neurons have a stronger response for moving stimuli (Cynader and Berman, 1972; Marrocco and Li, 1977). Moreover, a previous study has demonstrated modulation of fMRI response by attention to motion in human SC (Buchel et al., 1998). Thus, for retinotopic mapping within SC stimuli utilizing moving dots instead of contrast reversing checkerboards were developed. Stimuli are described in detail in Chapters III and IV.

EYE TRACKING

Eye movement data was collected using the ASL Eye-Trac 6000 (Applied Science Laboratory, Bedford, MA) eye tracking system outside the MRI scanner.

MRI METHODS

As mentioned in the previous chapter, functional BOLD imaging of the SC has previously been a challenge. Some ways to overcome these issues were suggested in a recent study (Wall et al., 2009), but work reported in this dissertation describes a novel set of acquisition and analyses approaches that may be used to perform fMRI of the SC (Katyal et al., 2012).

MRI acquisition methods

MR imaging was performed on a 3T scanner (GE Signa Excite HD) using the GE-supplied 8-channel head coil. Prior to collecting the functional experimental data, the acquisition protocols and parameters were optimized for imaging the SC.

T_2^* measurement for SC

Functional MRI measures task dependent blood oxygenation level dependent (BOLD) response. Measurement of the BOLD response depends on a tissue property called T_2^*, which is a time-constant for the dephasing of magnetic spins of protons (after providing them with an initial excitation and phase-synchronization). Since it is a tissue specific property, standard fMRI protocols optimized for the cortex, which has a $T_2^* \sim 48$ ms, may not yield the best signal in SC, which has different vascular, cyto- and myelo-architectural properties from cortex.

Therefore, separate T_2^* measurements were made for the midbrain neuroimaging work carried out in our lab. To make T_2^* measurements for SC tissue, resting state functional images were collected in human SC by varying the echo time, T_E, between 10 and 84 ms in five steps. Measured intensity data for each voxel at the various T_E values was then fit by the exponential:

$$M(t) = M_0 e^{-\frac{t}{T_2^*}}$$

The T_2^* for a region of interest (ROI) that covered the anatomical boundaries of SC had a value of ~65 ms, longer than the 48 ms typically observed in cortical gray matter. Accordingly, a proportionally longer echo time, $T_E = 40$ ms (30 ms is standard for cortex), was used during functional imaging to obtain stronger contrast.

Functional imaging

Eight 1.2-mm-thick quasi-axial slices (170-mm field-of-view) covered the entire SC with the prescription oriented roughly perpendicular to the local neuraxis. Each session consisted of multiple (for most sessions, 18) 228-s runs. The first 12-s of data was discarded to reduce transient effects.

A set of T_1-weighted structural images was obtained on the same prescription at the beginning and end of each functional scanning session using a 3D RF-spoiled GRASS (SPGR) sequence (15° flip angle, 0.78-mm pixels). In the high-resolution imaging work performed in our lab, we observe that subjects tend to show their largest motion early in each session. Therefore, the final set of the structural images was used to align and visualize the functional data (see following text). However, the MRI scanner available at our facilities had an issue of occasionally overheating and shutting down towards the end of a scan session. In case the scanner overheated before the second set of structural images were collected, the first set was used for subsequent analysis.

Functional MR imaging of the SC at 1.2-mm sampling requires a multi-shot acquisition. Acquisition time is limited by T_2^* decay to ~65 ms. For our scanner and FOV, a single-shot acquisition requires >77 ms even at peak bandwidth. Therefore, both two- and three-shot acquisitions were investigated in terms of both raw signal-to-noise ratio (SNR) and functional contrast-to-noise ratio. A low-bandwidth (62.5 kHz) three-shot acquisition worked best by both measures. Furthermore, a three-shot acquisition has a low-pass filtering effect, which is particularly beneficial for imaging the SC, since it reduces the high-frequency physiological noise corresponding to pulse and respiration.

Functional images were obtained on a prescription co-aligned with the above structural images. A 6.4-ms windowed-sinc pulse was used to provide a sharp slice-select resolution. A three-shot outward-spiral acquisition (Glover, 1999; Glover and Lai, 1998)

was used to obtain an inplane pixel size of 1.2 mm. Echo time, T_E = 40 ms, was used because of the correspondingly longer T_2^* of SC tissue compared to cortex. Acquisition bandwidth was limited to 62.5 kHz to reduce peak gradient current that caused unwanted heating on our scanner. A T_R = 1 sec was chosen, so with three shots, a volume was acquired every 3 sec.

The multiple shots were combined together after correction by subtracting the initial value and linear trend of the phase (Glover and Lai, 1998; Pfeuffer et al., 2002). Registration of the functional and structural images was generally very good, so *k*-space calibration of the gradients was unnecessary. Image reconstruction was done by gridding with a Kaiser-Bessel kernel using 2:1 oversampling. T_E was incremented by 2-ms on the first frame to estimate a field map from the first two volumes acquired, and this map was used for linear correction of the off-resonance image artifacts (Glover and Lai, 1998). Concomitant field effects arising during the readout gradients were also corrected by adding a time varying phase in the image reconstruction (King et al., 1999). Reconstructed images had an SNR of ~20. Temporal power spectra in SC voxels typically showed little of the structure associated with physiological noise; the use of a 3-shot acquisition had a strong filtering effect on the comparatively high-frequency effects of cardiac pulse and respiration.

Anatomical imaging

The structural images collected in each session were used to align the functional data to a high-resolution 3D reference volume anatomy, which was acquired for each subject in a separate session. The volume anatomy was T_1-weighted with good gray-white contrast, and was acquired using a 3D, inversion-prepared, SPGR sequence (min. T_E and

T_R, T_I = 450 ms, 15° flip angle, isometric voxel size of 0.6 or 0.7 mm, 2 excitations, ~28-min duration).

Image analysis

Analysis of the fMRI data was done using the mrVista software package (available for free download at http://white.stanford.edu/mrvista.php) as well as tools developed upon the mrVista framework in our lab. In-scan motion was estimated and corrected using a robust scheme (Nestares and Heeger, 2000). Because high-resolution data has relatively low SNR, motion correction was applied to a temporally smoothed (3—5-frame boxcar) version of the fMRI time-series data. Between-run motion was corrected using the same intensity-based scheme, this time applied to the temporal average intensity of the entire scan. The last run of the session was used as the reference. After motion correction, the many runs recorded during each session were averaged together to improve SNR. The intensity of the averaged data was spatially normalized to reduce the effects of coil inhomogeneity. The normalization used a homomorphic method, that is, dividing by a low-pass filtered version of the temporally averaged volume image intensities with an additive robust correction for estimated noise. Functional time-series data was then aligned and resampled to the reference volume anatomy using the robust intensity-based method applied to the structural images obtained for each session (Nestares and Heeger, 2000).

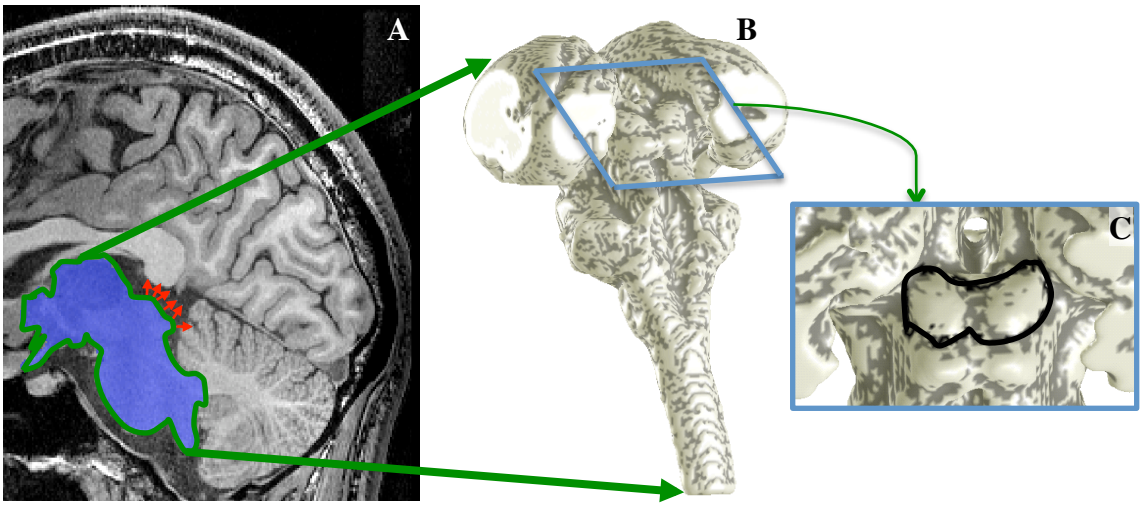

Figure 1: Segmentation and surface modeling. A) Portions of thalamus and brainstem including midbrain segmented from high-resolution MRI reference anatomy. B) 3D surface created at the edge of segmented region and smoothed. C) Rotated and enlarged view of the midbrain to visualize data on the SC (outlined in black)

Surface-based analysis

Within the high-resolution volume anatomy, portions of the thalamic and brainstem tissue including midbrain were segmented (Fig. 1A) using a combination of automatic and manual methods provided by the ITK-SNAP application (Yushkevich et al., 2006). The CSF-tissue interface of the SC was then interpolated from the segmentation using isodensity surface tesselation, and this initial surface was refined to reduce aliasing artifacts (Fig. 1B) using a deformable-surface algorithm (Xu et al., 2006). This surface provided vertices and outward normal vectors (Fig. 1A, red arrows), which were used as a reference for the depth-based analysis (described below) as well as a means to visualize the functional data (Fig. 1C).

A Euclidean nearest-neighbor distance map was calculated between the segmented tissue voxels and the vertices of the surface (Fig. 2). These distances were

used to measure depth position of the voxels within the reference volume relative to the CSF-SC tissue interface. Distances were positive inside the tissue and negative going out into the CSF. Functional data were aligned and resampled to the reference volume (Nestares and Heeger, 2000). Thus, each volume voxel was now associated with a complex response (magnitude, phase, and coherence) and a depth coordinate.

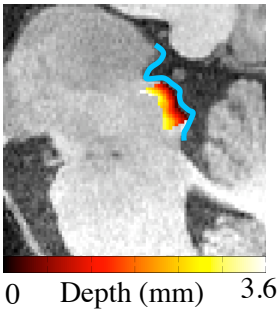

Figure 2: Distance map calculated between segmented tissue voxels in the reference volume and the vertices of the surface (blue). Colorbar below shows *depth* = 0 at the CSF-tissue interface and increases going into the tissue (only positive *depth* shown).

Depth profile calculation

For the experiments reported in Chapter III and V, the complex response and depth coordinate associations were used to calculate depth profiles of functional activity. Profiles were calculated within ROIs obtained from independent localizer sessions (described in more detail in the respective chapters). The coordinates of these ROIs at the SC surface were extended inwards and outwards along the surface normals obtained from the surface model. Within these extended regions, the complex response (magnitude and phase) as a function of depth was convolved with a boxcar-smoothing kernel (0.7-mm width); the magnitude of this convolution was the depth profile (Khan et al., 2011; Ress et al., 2007).

Bootstrapping techniques were used to obtain confidence intervals on the depth amplitude profiles in each subject and all subjects combined. For each ROI, the complex amplitudes were calculated for each run to create an ensemble of complex amplitude

datasets. Averages were then formed by resampling this ensemble with replacement over 5000 iterations, and calculating the depth profiles anew for each resampled average. Quantification metrics for comparison of different depth profiles are described within the method sections of individual chapters.

Depth averaging of data

In order to improve the quality of the data, a laminar segmentation process was performed that enabled averaging the time-series data in depth of SC. Small (0.5- or 0.7-mm-radius) disks of tissue were associated with each vertex of the surface model (Fig. 3A). Each disk was then extended both inward and outward from the SC tissue using the local surface normals (Fig. 3B) to form an individual laminar neighborhood (Ress et al., 2007). For each point on the SC surface, i.e., voxel nearest to each vertex, these associations were used to average the time series over a particular depth range. Coherence analysis was then performed on this multiple run averaged and depth-averaged time series to obtain model magnitude, phase and coherence values for each voxel before finally visualizing the data on the 3D surface representation (Fig. 3C, D).

For some of the experiments where a block design paradigm (Chapters IV and V) was used, the bivariate response metric of complex amplitude (magnitude with phase) was converted into a univariate metric by projecting the complex amplitude vector (combined magnitude and phase) upon a unit vector along a reference phase, which was calculated using high coherence activity corresponding to single (Chapter IV) or individual (Chapter V) blocks. Such a univariate amplitude metric contains positive values for data that lies within $\pm\pi/2$ radians of the reference phase and negative values for data that is out-of-phase.

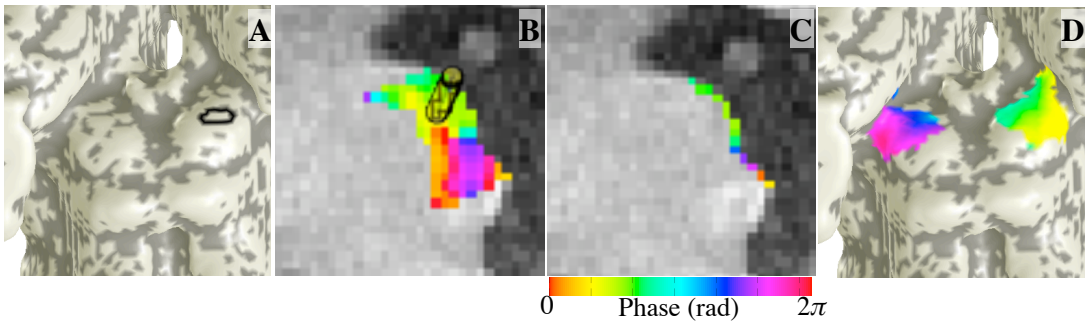

Figure 3: Laminar segmentation procedure for depth averaging. A) A disk of tissue associated with one of the vertices. B) Extension of the disk at the surface in depth of tissue (only inward extension shown here). C) Depth-averaged data. D) 3D surface visualization of data.

The noise in fMRI data is known to have a non-Gaussian distribution (Biswal et al., 1995; Glover et al., 2000; Holmes et al., 1997; Kruger and Glover, 2001). Typically, fMRI data is therefore "whitened" by performing a mixture of spatial and temporal blurring before statistical analysis (Friston et al., 2000; Worsley and Friston, 1995). To maintain the high spatial resolution for these experiments, there was a need to avoid such blurring. Therefore, non-parametric methods were used to estimate statistical significance of these models. For coherence analysis, significance was estimated for each voxel by regressing the model sinusoid obtained from the magnitude and phase of the depth- and session-averaged data upon bootstrapped averages of individual run time-series (resampling with replacement time-series from the many individual runs and taking their average) over 10,000 iterations. The *p*-value was then the fraction of this bootstrapped regression data following the null hypothesis that the regression slopes were negative. For the univariate amplitudes, significance was estimated by bootstrapping the univariate amplitudes (calculated by projecting the bivariate complex amplitudes upon a reference phase) for each voxel for the many individual runs over 10,000 iterations. The *p*-value

was then the fraction of resampled data <0 for voxels that had a positive mean amplitude (in-phase) and >0 for voxels that had a negative mean amplitude (out-of-phase data).

Direction and reliability of phase gradient

The surface of the SC was flattened using standard approaches (Wandell et al., 2000) and the depth-averaged phase data was transformed from reference volume to this flattened representation. This flattened 2D view was used to calculate the direction and reliability of the retinotopic phase progressions.

Direction of phase progression was calculated by evaluating the spatial gradient of the phases (Silver et al., 2005) for each of the stimulation and attention maps. Horizontal and vertical components of the gradient were calculated using the depth-averaged complex amplitudes for each pixel on the flat view. The horizontal component of a pixel was the mean difference of complex amplitudes for the three neighboring right pixels with those on the left, and the vertical component was the mean difference of complex amplitudes for the three neighboring pixels above with those below. Direction of each pixel was then calculated as the inverse tangent of the ratio of the angle of the complex number at each pixel for the vertical component to the horizontal component. Overall, direction of each map was calculated as the mean direction of pixels within the independent ROIs described for the respective experiments in Chapters III and IV.

The horizontal and vertical components were also used to calculate the statistical significance of each phase gradient, testing the hypothesis if a phase gradient was reliably present along the direction indicated by the experimental results. Dot products were calculated between the vectors formed by combining the horizontal and vertical components for each individual runs upon the mean vector and these dot products were

bootstrapped over 10,000 iterations. The *p*-value was then fraction of the dot product magnitudes <0.

Chapter III: Polar-angle representation of visual stimulation and attention in SC

The experiments described in this chapter have been previously published in the *Journal of Neurophysiology* (Katyal, S., Zughni, S., Greene, C., and Ress, D. (2010) Topography of covert visual attention in human superior colliculus. No. 104, Pages 3074-3083). In terms of contributions from the other authors, Samir Zughni assisted in performing some of the pilot work for these experiments including programming an earlier version of the visual stimulus, while Clint Greene undertook the process of segmenting the brainstems in the reference volumes for four out of five subjects. Dr. David Ress was the supervisor for these experiments as well as the principal investigator for the grant NSF BCS 1063774, which funded this work.

The retinotopic organization of visual stimulation signals has long been known to exist in the non-human primate SC (Cynader and Berman, 1972; Goldberg and Wurtz, 1972a) and has more recently been demonstrated in humans using fMRI (Schneider and Kastner, 2005, 2009). Here I make these fMRI measurements in humans using a higher spatial resolution; a factor of 2.6 times smaller than the previous fMRI studies. Then I show that visual attention signals are also topographically organized in a similar orientation and are spatially in register with the visual stimulation signals.

I also measure the depth profiles of visual stimulation and attention signals. For this goal, separate fMRI sessions were collected using a lateralized blocked-alternation protocol for both stimulation and attention, in order to maximize the duty cycle. The fMRI response for both visual stimulation and attention occurred close to the superficial surface of SC, with stimulation response having a significantly wider profile than attention, thereby protruding deeper into the colliculus.

METHODS

Subjects

Five subjects performed several two-hour-long scanning sessions: 1—2 stimulation retinotopies, 1—2 attention retinotopies. Four of the five subjects performed one lateralized stimulation, and two lateralized attention sessions each.

Three subjects (two of which had participated in the fMRI experiments) participated in separate stimulation and attention psychophysics sessions outside the scanner while their eye movements were monitored.

Visual stimulus protocols

All experimental scanning session reported in this chapter utilized the back-projection display (#1 described in Chapter II).

Polar angle representation of visual stimulation

Stimulus was a 90° sector of radially moving black and white dots (4°/s speed), eccentricity 2—10°, which was subdivided into 2 × 3 virtual sections (Fig. 4A). The task of the subjects was to discriminate if dots in one of the sections were moving at a speed faster or slower than dots in the other sections, while maintaining fixation. The sector of moving dots was displayed at each polar angle location for a 2-sec trial period, and subjects were required to make a response by pressing one of two buttons indicating their judgment of faster or slower within the last 0.5-sec of the trial period. Subjects were instructed to maintain attention at the moving dot sector and be as accurate as possible. The sector then rotated by the width of one virtual sector (30°), and the trial was repeated. The radial direction of the dots alternated between inward and outward after each trial to prevent adaptation. The entire stimulus rotated 9.5 times around fixation with a period of 24 seconds. Task performance of the subjects was maintained at >71% by continually

adjusting the magnitude of the speed difference between dots in the faster or slower section relative to the other dots in the sector using a pair of randomly interleaved two-up-one-down staircases. After every two consecutive correct trials the speed difference was reduced by 8% and for every incorrect trial the difference was increased by 8%.

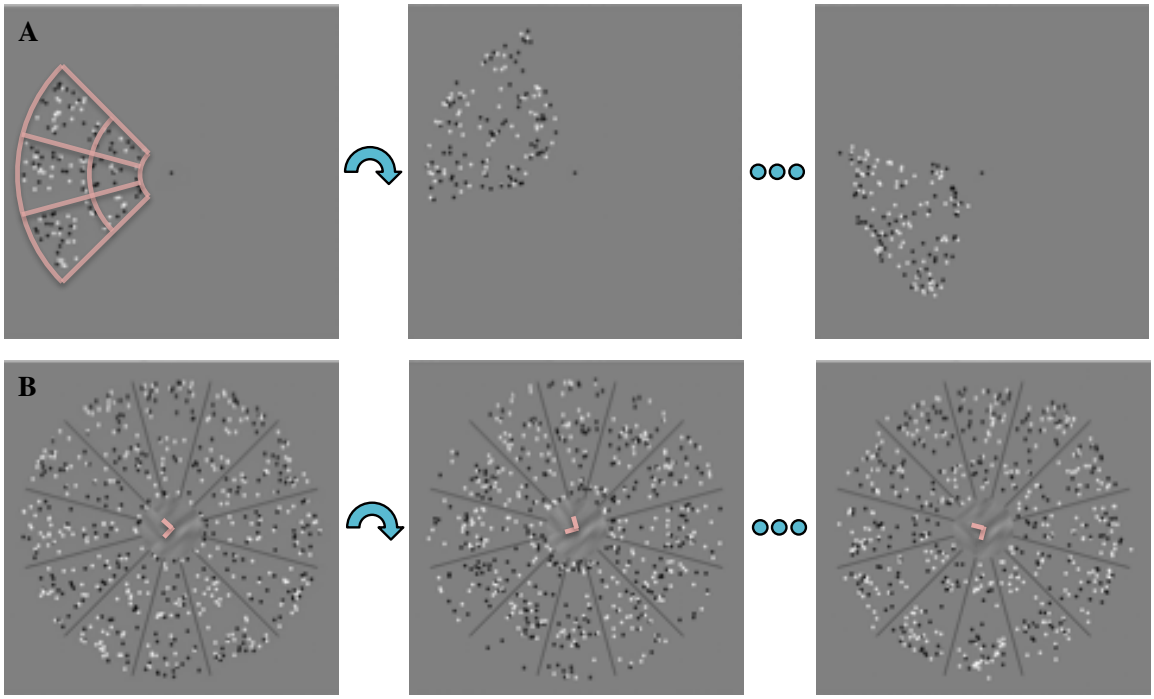

Figure 4: Polar angle retinotopic mapping stimuli. A) In the visual stimulation experiment, a 90° sector of moving black-and-white dots on a gray background rotated slowly around fixation. The sector was divided into 6 virtual sections (pink lines added in figure) to enable the subject to perform a speed discrimination task in a random section. B) In the visual attention experiment, the stimulus was a full field of similar moving-dots with constant spatial distribution. Subjects were cued by thin black lines near fixation (emphasis added in figure) to perform a similar speed-discrimination task within a 90° sector.

Before the scanning sessions, subjects practiced the task outside the scanner for 2—3 20-min training sessions until their performance stabilized. The initial speed

difference was based upon their performance during these training sessions, and was typically 1—2°/s.

During fMRI scanning sessions, subjects performed this task over the course of multiple ~4-min-duration runs. The discontinuity introduced between runs tends to slightly disorient subjects. This was dealt with by starting subsequent runs with a speed difference 1.5 times the mean speed difference calculated during the latter half of the previous run. This easing of difficulty permitted subjects to quickly reorient to the task strategy and their performance then tended to rapidly return to their respective thresholds after ~30—40 trials in a stereotypical fashion that repeated well from run to run.

Polar angle representation of visual attention

Stimulus was a full field (eccentricity 2—10°) of similarly moving dots divided into 2 × 12 virtual sectors. A pair of orthogonal cue lines (length, 0.08°) extending from fixation directed attention of the subject to a 90° sector-shaped aperture (same as for visual stimulation) within the stimulus (Fig. 4B). The cue rotated around fixation (24-s period) and subjects performed a similar speed discrimination task in the cued aperture. To counterbalance the speed difference in the cued aperture, a speed increment or decrement was also present in one of the sections within a 90° sector directly opposite to the cued wedge. Subjects' performance was adjusted using a similar staircase procedure as described previously.

Lateralized stimulation and attention

To obtain laminar profiles, lateralized stimulation and attention stimuli were used to maximize the duty cycle of the functional response. For the lateralized stimulation condition, stimulus was a 144° polar angle and 2—10° eccentricity sector of moving dots that alternated 9.5 times between the left and right visual fields with a 24-s period (Fig.

5A). The sector on each side was subdivided into 2 × 4 virtual sections and task of the subjects was, once again, to discriminate if the dots in one of the sectors were moving faster or slower than dots in other sectors. Trials again had a 2-sec duration, with six trials on each side. The data from lateralized stimulation was also used as an independent localizer for the stimulation and attention retinotopy experiments.

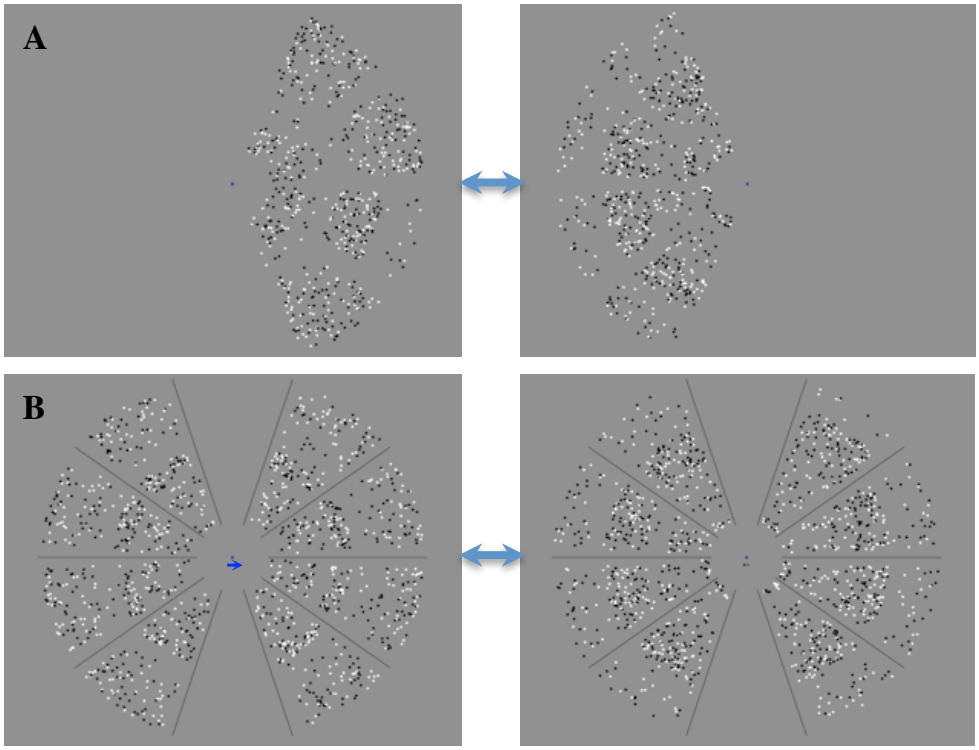

Figure 5: Lateralized visual stimulation and attention stimuli. A) For lateralized stimulation a 144° polar angle and 2—10° eccentricity sector of moving dots along the horizontal axis alternated between right and left hemifields in 12-sec blocks. Subjects fixated and performed six dot speed discrimination task in one of 8 virtual sections within each. B) For lateralized attention, similar sectors on both sides were presented. A tiny arrow below fixation mark (emphasis added in figure) cued attention to left and right in alternating 12-sec blocks. Subjects performed the same task.

For the lateralized attention condition, the stimulus had moving-dot sectors on both left and right sides with an arrow below the fixation mark cueing the side to be

attended (Fig. 5B). Subjects performed the same task as in the lateralized stimulation condition. In addition, during the last trial on each side, the fixation dot changed color, warning the subject that attention should be switched on the next trial.

Eye Movements

Three subjects participated in six 216-sec runs each of the stimulation and attention stimuli while eye movement data was collected outside the scanner. Time series of horizontal and vertical gaze coordinates as well as the pupil diameter were acquired at a sampling rate of 60 Hz. In order to examine eye movements each eye-position measurement was projected onto a unit vector in the direction of the target or cued region, yielding a large ensemble of measurements (~12,000, after taking valid pupil and corneal reflection recognition into account). The mean of this measurement quantifies the bias of eye position in the target direction, which can be compared to the mean eccentricity of the target region. This comparison was repeated for saccade vectors extracted from the eye-position data to also test for bias in saccadic eye movements.

MRI acquisition methods

MRI acquisition procedures were the same as those described in Chapter II (General methods).

Image analysis

The image analysis was performed in the manner described in Chapter II. For both the retinotopy and block design experiments, data was averaged over a depth of 0—1.8 mm. For visualization, the phase values of the depth-averaged data were overlaid upon the SC surface (Fig. 6).

In order to quantify the retinotopy data, independent ROIs were defined for each subject using the depth-averaged lateralized stimulation data, which served as an

independent localizer. ROIs were defined manually by choosing a contiguous region consisting of the most responsive portion within the collicular surface. Specifically, ROIs were defined for each subject by adjusting the coherence threshold for each subject within the range 0.30—0.50, so that a similar surface area was included, ~23 mm^2. These ROI boundaries are marked using black dotted lines in Fig. 6. The direction the retinotopic phase progression (described in Chapter II) was calculated within these ROIs. Rough boundaries were also obtained of the entire superficial extent of the SC using manual inspection of the high-resolution T_1-weighted volume anatomy. These boundaries are marked in Fig. 6 by red dashed lines.

Registration of stimulation and attention retinotopies

To test the registration of the visual stimulation and attention maps, correlation analysis was performed within the localized ROIs described above, between phase-values obtained for the attention retinotopies against those obtained for the visual stimulation retinotopies. Phase values for each session were corrected by subtracting an estimate of the hemodynamic delay. This estimate was calculated for each subject as the mean phase of the data within ROIs for both colliculi in the complex plane, and then subtracting π. Such a metric is based on the assumption that the phases between the two colliculi are lateralized and therefore in case of no delay their mean phase would be π. Hemodynamic delay values were small, in the range of 1.5—4 s. Mean hemodynamic delay, averaged across all subjects for both attention and stimulation conditions, was 2.9 sec; the color pinwheel in Fig. 6 has been rotated accordingly.

Bootstrapping was used to obtain confidence intervals on the correlations for each subject and all subjects combined. For each attention session, a run-by-run ensemble of depth-averaged complex amplitude datasets was calculated. Then correlation analysis

was performed with the retinotopy data for 5000 averages of the attention runs, each average obtained by resampling the ensemble with replacement. The p values corresponded to the fraction of the correlations yielding a fit with slope ≤ 0.

Depth profile calculation

The general procedure for depth-profile calculation has been described in Chapter II. Because SC has a variable thickness across its lateral-medial extent, three 3-mm-diam ROIs were defined to cover activated regions on lateral, central, and medial portions of each SC (Fig. 7A). The active portion of the SC was ROIs from the lateralized stimulation sessions described above. In each of the three ROIs for every subject, the complex amplitude as a function of depth for all runs averaged together was obtained. In order to correct for hemodynamic delay, phase normalization was performed for each run by dividing the complex amplitude of the profile with the mean phase within the respective ROI restricted to the collicular surface where the data was strongest and most reliable. Depth profiles for attention and stimulation were normalized to unity for ease of comparison. Profiles obtained without correction for the hemodynamic delay were qualitatively similar but less reliable.

Centroids of the depth profiles were calculated to quantify a comparison between attention and stimulation:

$$c = \frac{1}{\hat{A}} \int_{s_{min}}^{s_{max}} sA(s)ds \,,$$

where $A(s)$ is the amplitude as a function of depth and $\hat{A}$ is the average amplitude. The integration limits s_{min} and s_{max} were set to 0 and 3.5 mm, respectively, which is roughly the thickness of human SC. The centroid calculation was also bootstrapped across the ensemble of runs to obtain confidence intervals.

RESULTS

Behavioral performance

All subjects were able to successfully maintain accuracy at >71% during each session. For the stimulation and attention retinotopies, average performance was 81% and 82% respectively. Discrimination thresholds were somewhat better for the attention retinotopy condition (1.0°/s) than the stimulation retinotopy (1.2°/s); this difference was significant (negligible p) in three of the five subjects. Performance was slightly better for lateralized stimulation and attention conditions, 85% and 82% respectively, with discrimination thresholds of 1.2 and 1.1°/s, respectively and not significantly different for all four subjects ($p > 0.4$). The lower thresholds for the attention condition suggest that some subjects were able to perform the purely attentional task more effectively than the stimulation (with attention) task, possibly because the latter task does not permit full usage of covert attention resources.

Polar angle representation of visual stimulation

For all subjects, visual stimulation data was reliably lateralized, i.e., phases corresponding to the left visual field stimulation were observed in the right colliculus and those corresponding to the right visual field in the left colliculus (Fig. 6A). Amplitudes of the MR signal were typically between 0.1—0.2%, except for subject 4, who was an unusually strong responder (Table 1).

Retinotopic progression of the data was tested by calculating phase gradients, indicated by dark arrows under each individual colliculus in Fig. 6A along with their bootstrapped 68% confidence range indicated by the two brown arrows. The phase gradients were statistically significant ($p < 0.05$) in 8/10 individual colliculi (subjects 1, 3 and 4 bilateral, subject 2 and 5 left) and were between 93—95% confidence for the other

two colliculi. Retinotopic phase gradients were also highly significant ($p \sim 0$) in the group data. In 5/10 colliculi, there was a reliable anterior-posterior tilt to the retinotopic maps, from rostro-medial through caudo-lateral (subject 4 bilateral, subjects 1, 5 right, subject 2 left) going from upper to lower visual field. The phase progression in the right colliculus of subject 2 was oriented in an anterior-posterior direction.

On visual inspection, 8/10 colliculi were seen to have a nearly complete polar angle retinotopic map of visual stimulation (subjects 3—5 bilateral, subjects 1—2 right). The top half of the contralateral visual field was represented medially (blue in the left colliculus and cyan/green in the right colliculus) and the bottom half was represented laterally (pink/magenta in the left and yellow in the right colliculus). There was an over-representation of phases corresponding to the horizontal visual field in the colliculi as compared to the vertical visual field, with a particular paucity of phases near the lower vertical meridian.

Polar angle representation of visual attention

As in the visual stimulation condition, phases corresponding to visual attention were also reliably lateralized in all subjects (Fig. 6B). Amplitudes of the attention signals were smaller than the stimulation signals, typically between 0.05—0.13% (Table 1).

In 4/10 colliculi, the phase-gradient calculations indicated a reliable ($p < 0.05$) medial-to-lateral organization of attention signals (subjects 3—4 bilateral). When the phase gradient data was analyzed across all subjects, it was highly significant ($p \sim 0$) for both left and right colliculi.

On visual inspection, phase progressions in 7/10 colliculi gave the appearance of retinotopic maps with a medial-to-lateral organization of phases corresponding to the

upper and lower contralateral visual fields respectively, similar to the stimulation maps (subjects 1, 4, and 5 bilateral; subject 3 left).

	Stimulation amplitudes (%)		Attention amplitudes (%)		Attention-stimulation correlations, R^2			Attention-stimulation slope		
Subject	Left	Right	Left	Right	Left	Right	Both	Left	Right	Both
1	0.14	0.09	0.07	0.05	0.26	*0.93	***0.77	1.89	0.63	0.89
2	0.07	0.17	0.09	0.05	0.41	0.22	*0.72	0.94	0.20	1.01
3	0.16	0.10	0.09	0.09	*0.78	0.26	***0.89	0.84	0.12	0.69
4	0.52	0.64	0.13	0.11	**0.72	*0.75	***0.97	0.68	1.02	0.92
5	0.15	0.13	0.09	0.10	*0.55	***0.95	***0.97	1.07	0.96	1.18
All					***0.32	***0.56	***0.80	0.45	0.40	0.78

Table 1: Stimulation and attention amplitudes (percent modulation) and correlations (significance: $*p < 0.05$, $**p < 0.005$, $***p < 0.0005$) for each colliculus in each subject.

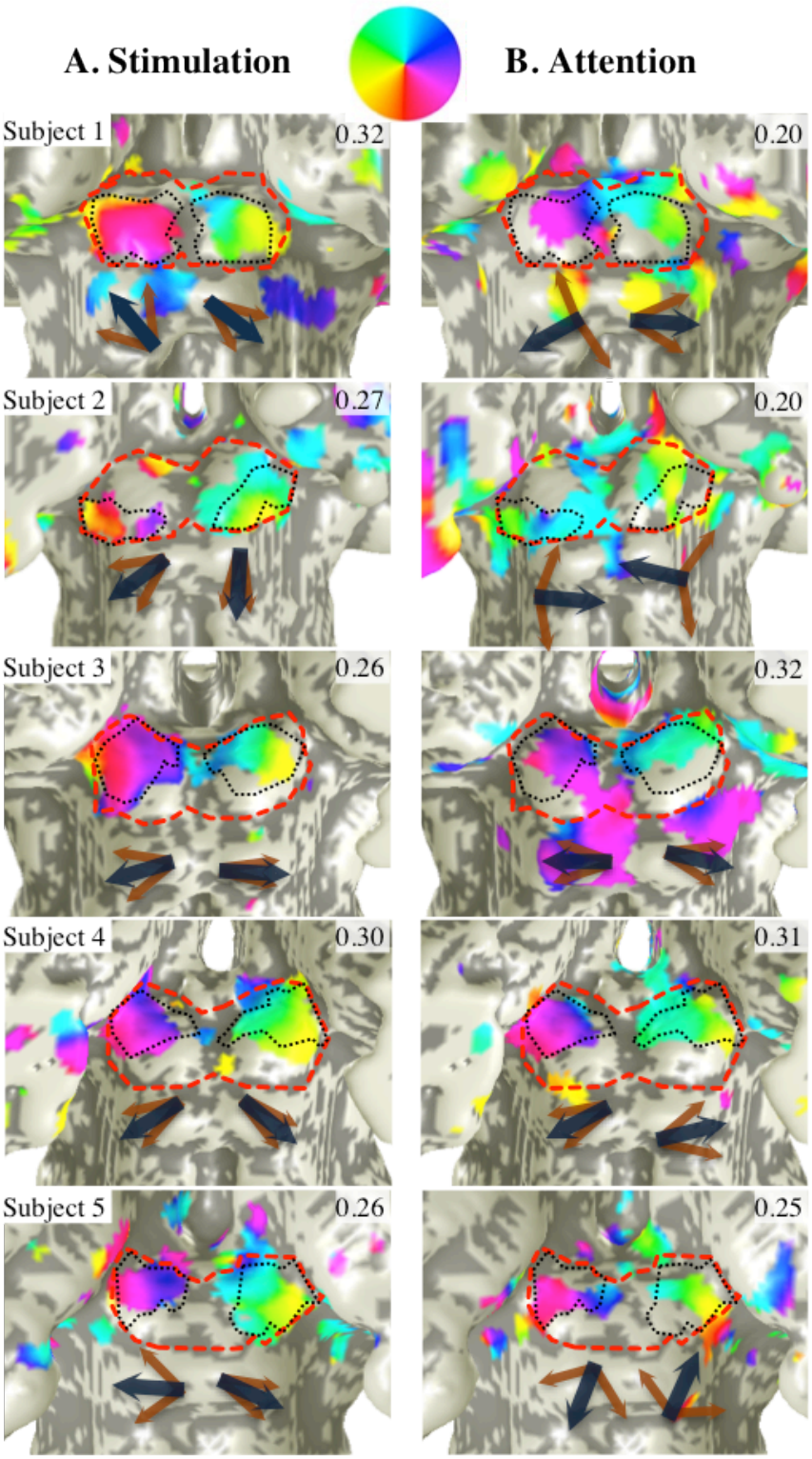

Figure 6: Polar angle retinotopic maps. fMRI phase maps in five subjects; left column shows maps of stimulation, right column of attention. The color wheel shown near top relates the overlaid phases to their visual field positions. Black arrows under each colliculus depicts the direction of phase gradient from upper to lower visual field. Brown arrows indicate 68% confidence intervals of the phase gradients.

Registration of visual stimulation and attention

If human SC did indeed contain retinotopic maps of stimulation and attention, then based on monkey literature they would be expected to be in spatial registration. Therefore, testing this registration provides another measure of the validity and reliability of the observed spatial distributions. In order to quantify registration, correlations were performed between the visual stimulation and attention polar-angle phase data within the same depth-averaged regions. Statistical significance of these correlations was assessed non-parametrically using bootstrapping (see Methods). Correlations with both colliculi of a subject analyzed together were large (typically $R^2 = 0.72—0.97$) and significant ($p \sim 0$) for all subjects indicating strong and reliable lateralization of the SC responses. For individual colliculi correlations ($R^2 = 0.55—0.95$) were significant ($p < 0.05$) in 6/10 colliculi (Table 1).

Figure 7A shows correlation results for a representative single subject (left: $R^2 = 0.78$, $p = 0.02$; right: $R^2 = 0.26$, $p = 0.22$; together: $R^2 = 0.89$, $p \sim 0$). For all subjects combined (Fig. 7B), correlations were strong (left: $R^2 = 0.32$; right, $R^2 = 0.56$, together: $R^2 = 0.80$) and highly significant for both individual and combined colliculi ($p \sim 0$).

Slopes of the fits between attention and stimulation were less than unity in three of the colliculi that showed significant correlations between stimulation and attention, as well as the group-averaged data (Table 1).

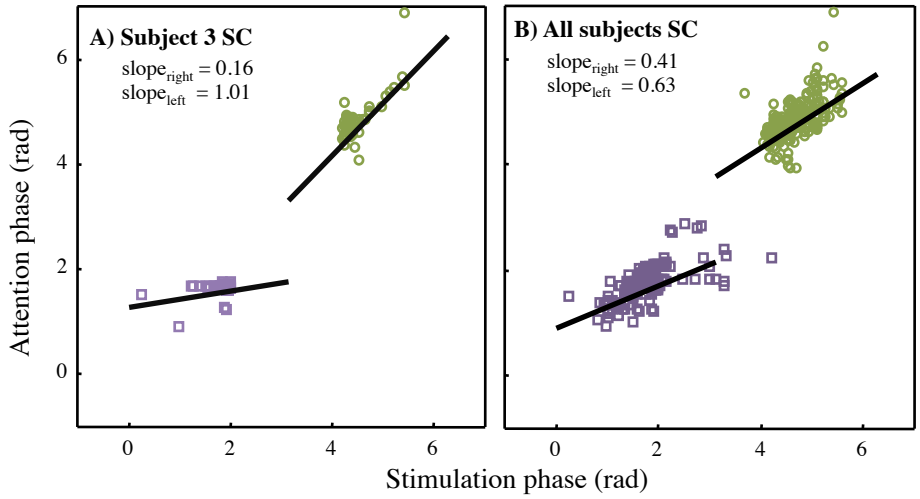

Figure 7: Phase correlations. A) Phase values obtained for left (purple) and right (green) SCs in the attention experiment plotted against phase values obtained in the stimulation experiment for subject 3. Slope of the fits are indicated on the graph. B) Similar plot for five subjects combined.

Eye movements

To ensure that subjects were able to maintain fixation for the stimulus as instructed eye tracking was performed on three subjects in separate sessions outside the scanner. The projected component of eye position along the cued polar angle of the stimulus was calculated. This projection value was typically very small with mean across subjects of 0.06° and –0.01° of visual angle for attention and stimulation conditions respectively. Though the attention projections were significant ($p < 0.05$; two tailed t-test) due to the large number of samples (~12000), they were still minute compared to the 5° mean eccentricity of the stimulus. The infrequent saccades that the subjects made were also extracted from the eye position data and their component along the stimulus polar angle was analyzed; the mean values were small, <0.1° and statistically indistinguishable from zero for all but one subject in the stimulation condition (mean ~0.3°, $p<0.01$). Thus, for the most part eye movement errors were random without significant bias toward the

target aperture, and in the case they were directed toward the stimulus their length was too small to affect the spatial extent of activity on the SC surface.

Depth profiles of stimulation and attention

In order to evaluate laminar activity profiles of stimulation and attention, three ROIs were chosen for each colliculus: lateral, central and medial (Fig. 8A). Depth profiles for the left colliculus of subject 4 (Fig. 8B) show the typical character of the data, which reached a peak near the superficial surface of the colliculus and decreased with increasing depth. No significant left-right or subject-to-subject differences were observed in the profiles, so the obtained profiles were averaged across both colliculi in all subjects (Fig. 8C) to improve statistical power. Stimulation and attention depth profiles were normalized to unity to facilitate visual comparison between the profiles. The activity was distinctly superficial for both stimulation and attention, generally evident only for $d < 2$ mm, with much less activity for $2 < d < 4$ mm. The medial and central profiles were ~32% thinner than the lateral profile, which is consistent with the anatomy of SC (Paxinos and Mai, 2004; Tardif and Clarke, 2002). Depth profiles for the lateral and central ROIs showed that activity for visual stimulation extended deeper into the colliculus than for the attention. This difference of depths as measured by the centroid of distribution over a depth of 0—3.5 mm was significant for both the lateral and central ROIs (centroid differences: lateral, 0.31 mm, $p = 0.0002$; central, 0.22 mm, $p = 0.016$; medial, 0.09 mm, $p = 0.20$). For both conditions, the superficial activity extended outside of the SC ($d < 0$), probably because of the presence of superficial blood vessels. Since the depth of the colliculus is variable, centroids over depth ranges of 0—3 (lateral, 0.30 mm, $p \sim 0$; central, 0.15 mm, $p = 0.027$; medial, 0.05 mm, $p = 0.26$) and 0—4 mm (lateral, 0.34 mm, $p = 0.0014$; central, 0.24 mm, $p = 0.04$; medial, 0.14 mm, $p = 0.15$) were also

calculated and found that the differences in centroids for the lateral and central ROIs had similar absolute values that remained significant.

At a coherence threshold of 0.30, ~40% of the colliculus showed activity corresponding to the lateralized stimulation condition, which had a maximum eccentricity of 10°. This is roughly consistent with monkey stimulation maps that have shown that a third of the colliculus is represented for the central 10° of the visual field (Cynader and Berman, 1972).

DISCUSSION

The amplitudes of responses were slightly higher for the stimulation than the attention data (Table 1). Data quality in SC for the attention condition was slightly worse than stimulation, which is why two attention runs were averaged for three of the five subjects. The noise levels in the phase data are not surprising, given the very small amplitudes of signals observed in this study.

There was a topographic progression of signals along polar angle corresponding to visual stimulation in the SC of 8/10 colliculi, thus confirming the presence of retinotopic maps of polar angle in human SC. The orientation of these maps was consistent with the visual stimulation and eye movement maps obtained in monkeys (Cynader and Berman, 1972; Robinson, 1972) as well as those obtained in a previous fMRI study in humans (Schneider and Kastner, 2005).

In at least 4/10 individual colliculi, and in the group data, covert visual attention signals also progressed topographically, indicating the presence of polar angle retinotopic maps of visual attention in human SC. Visual inspection gave the appearance of similar patterns of phase progression between the attention and stimulation maps (Fig. 6).

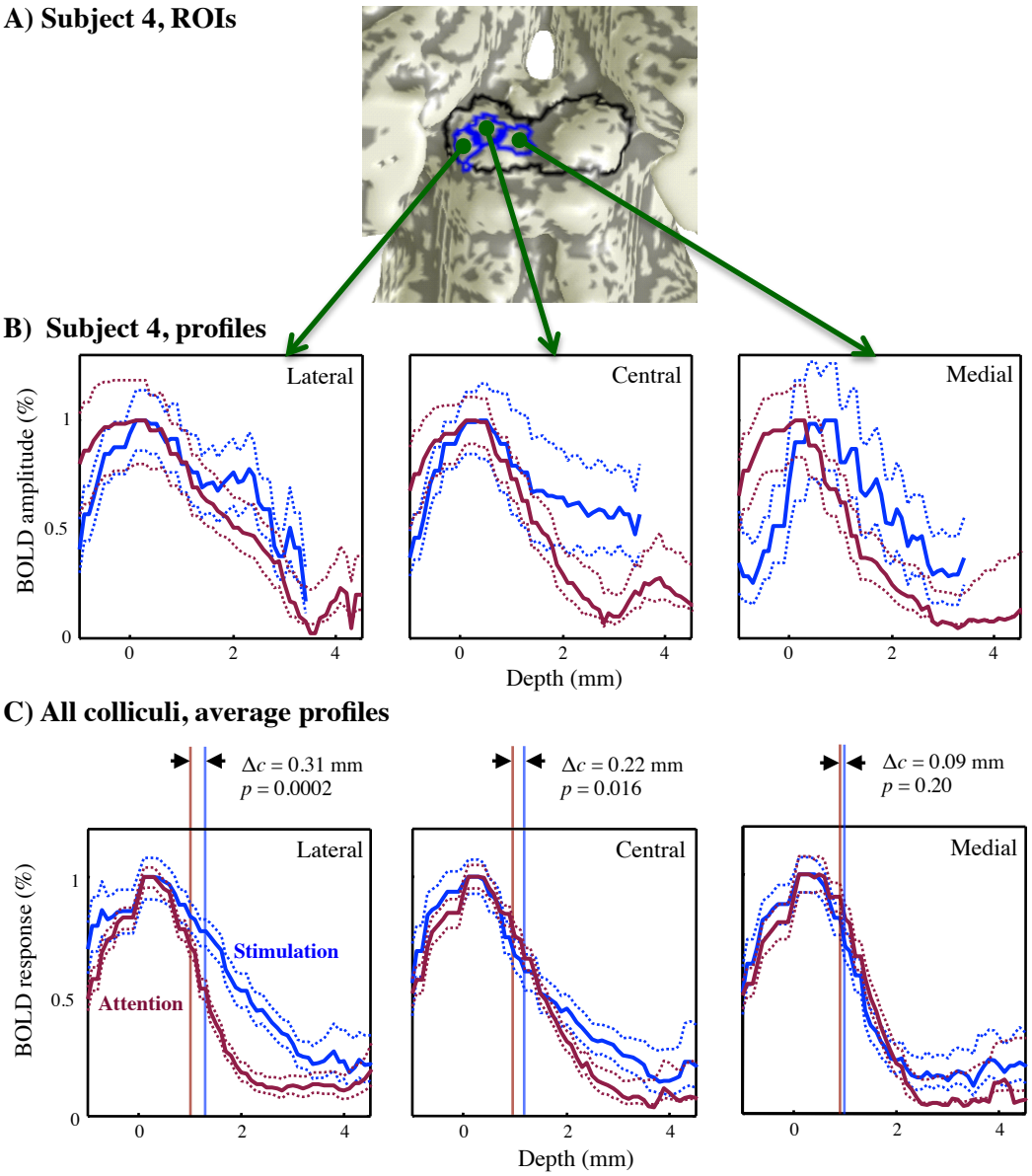

Figure 8: Laminar profiles. A) Outlines of lateral, central and medial ROIs for subject 4. B) Laminar profiles for subject 4, left colliculus. Thick lines are the mean profiles (stimulation in blue; attention in maroon) and the thin dotted lines indicate 68% confidence intervals. C) Laminar profiles averaged for all subjects over both colliculi showing centroid differences between the attention and stimulation profiles.

Phase correlations in the individual colliculi between the polar angle stimulation and attention conditions supported the presence of a retinotopic map of visual attention in SC (Fig. 7). Good correlations were obtained in 7/10 individual colliculi, though the individual slopes were typically less than unity (Table 1). The correlations obtained for both colliculi together were strong and had near-unity slope, demonstrating that visual stimulation and attention signals were similarly lateralized.

The intermediate layers of the SC contain neurons that respond retinotopically to eye movements. Since, eye movements were not tracked during our scanning sessions, it is possible that the stimulation and attention maps may have been partly confounded by subjects' eye movements. However, eye movements were tracked in separate sessions outside the scanner and showed that the subjects were able to successfully maintain fixation while performing the visual stimulation and attention tasks.

Slopes of less than unity were observed in some of the phase correlations between the attention and stimulation conditions in SC. Taken literally, this would indicate a more compact distribution of attention phases compared to stimulation, possibly because of a weaker response along the vertical meridian for attention as compared to simulation. However, for individual colliculi the slope increased with the R^2 value, i.e., more strongly correlated data have slopes closer to unity. This suggests that the observation of slopes < 1 may be an artifact caused, for example, by small misalignments between the attention and stimulation runs, or by additional noise in the attention data causing phase wrapping.

Depth profiles for visual simulation and attention both showed that activity reached a peak near the superficial surface of the SC, and then gradually decreased with increasing depth. Activity was greatest at depths <2 mm, corresponding most likely to the superficial and intermediate layers of the SC that contain visual and oculomotor neurons respectively.

Alternatively, it is possible that because oxygenated blood is delivered and recovered superficially, depth profiles of BOLD activity may not have a one-to-one spatial correspondence to local neural activity; activity in deeper regions may simply be less hemodynamically evident than superficial activity. A similar tendency for hemodynamic activity to peak near the superficial tissue surface has been previously observed in cortical gray matter (Harel et al., 2006; Lu et al., 2004; Ress et al., 2007).

Irrespective of the explanation of the superficial nature of the depth profiles, the centroids of activity were observed to protrude significantly more deeply into the colliculus for visual stimulation than attention, possibly suggesting the presence of visual activity in the deeper layers of SC that was not modulated by attention (Fig. 8).

Evidence from single-unit neurophysiology studies has suggested that there is an enhancement of activity in the superficial and intermediate layers due to attention (Cavanaugh and Wurtz, 2004; Goldberg and Wurtz, 1972b; Ignashchenkova et al., 2004). The depth activity observed in our profiles is consistent with these studies. However, there may be at least two possible explanations for deeper presence of the visual stimulation response compared to attention.

First, in addition to the visually responsive neurons in the superficial and intermediate layers, there are also visually responsive uni- and multi-modal neurons in the deep layers of SC (Wallace et al., 1996). The deeper fMRI response for visual stimulation would suggest that these deeper visually responsive neurons are not being modulated by attention. So far, no electrophysiology studies have reported attentional modulation of these deeper sensory signals, typically arising from cortical association areas.

The only other difference between the lateralized visual stimulation and attention stimuli was the central cue. So a second reason may be that the depth differences were

driven by this difference in stimuli. This is extremely unlikely considering that the cue was present in the attention condition, which actually had the shallower of the two profiles. Moreover, the size of the cue was very small (0.08°) compared to the extent of the stimulus (2—10°). Based on the retinotopic organization of visual stimulation it is unlikely that the ROIs within which depth profiles were analyzed were contaminated by the cue. Hence, the differences in profiles between the stimulation and attention conditions were probably not an artifact of the cue manipulation.

All in all, these results provide further details about the presence and nature of visual attention in human SC, buttressing a long history of research. Visual attention related modulation has been observed in the SC both monkeys (Goldberg and Wurtz, 1972b; Ignashchenkova et al., 2004; Wurtz and Mohler, 1976) and humans (Buchel et al., 1998; Schneider and Kastner, 2009). Monkey microstimulation studies have shown a spatially specific enhancement of performance in visual tasks indicated a spatiotopic organization of visual attention in the SC (Cavanaugh and Wurtz, 2004; Muller et al., 2005). The results presented in this chapter have extended this work by demonstrating that the organization of cue-evoked attention in humans is also spatially specific and conforms to the retinotopic of the visual signals, at least along the polar angle direction.

In summary, a reliable lateralization has been demonstrated and, in some subjects, with a retinotopic organization of visual attention signals in human SC. The attention-evoked activity specifically boosts responses in what seem to be the superficial to intermediate layers of SC. Thus, attentional signals seem to be both in retinotopic and laminar registration with the neural substrates for eye movement preparation and generation. Our findings are in support of a visuomotor basis for visual attention, in accordance with the notion that attention mediated signals are present in the same neural substrates that control eye movements and other orienting responses (Moore and

Armstrong, 2003; Rizzolatti et al., 1987; Rizzolatti et al., 1994). A more detailed analysis of attention signals and their correspondence to the visuomotor theory of attention is presented in Chapter V of this dissertation.

Chapter IV: Eccentricity representation for visual stimulation and attention in SC

In the second set of experiments, I measured the topographic organization of visual stimulation and attention in SC along the eccentricity dimension. A previous fMRI study, which showed the polar angle representation of visual stimulation in human SC, also attempted to measure the representation of eccentricity but was unsuccessful in doing so (Schneider and Kastner, 2005). There could have been several reasons for this. 1) The maximum eccentricity covered in their visual stimulus was 15°, which in macaque maps covers approximately half the SC (Robinson, 1972). Their spatial resolution (1.5 × 1.5 × 2 mm^3) might not have been enough to resolve an eccentricity representation within such a small region. 2) The stimulus used in that experiment was based on the conventional contrast-reversing checkerboards, which may not have been optimal for evoking visual stimulation signals in the SC. 3) Because fMRI responses in SC are substantially modulated by behavior (Katyal et al., 2010; Schneider and Kastner, 2009), their paradigm which involved passive visual stimulation may not have produced a statistically observable fMRI response. 4) Eccentricity may be a more difficult BOLD measurement to make compared to polar angle due to vascular differences between the rostral-caudal and medial-lateral axes 5) And finally, though much less likely, visual stimulation signals might not be organized topographically within human SC along eccentricity.

The experiments reported here take into account some of the above factors by 1) using a higher spatial resolution, 2) using an increased field of view (FOV) of the visual stimulus (30° along eccentricity), 3) using a moving dot stimulus, and 4) having subjects performing an active behavioral task within the stimulus aperture.

In order to measure the organization of visual attention signals along eccentricity, a two-eccentricity block-design stimulus was used instead of a phase-encoded scheme. This was done in order to maximize the duty cycle of the stimulus because, 1) of the low SNR observed in eccentricity measurements made during preliminary experiments, and, 2) deploying attention at large eccentricities (~25°) was found to become increasingly more difficulty in the presence of task relevant distractors at inner eccentricities.

METHODS

For eccentricity measurements the back-projection screen (display #1, described in Chapter II) was used as it had a maximum FOV of 31° along the horizontal. Instead of the using standard bilateral stimulation approach with the center of the screen as fixation, which would halve the FOV for a single hemifield, these experiments were performed unilaterally, utilizing the full FOV for that hemifield. Subjects were asked to rotate their heads and fixate at one edge of the screen while visual stimuli were presented within a hemifield. Such a stimulus was expected to evoke a response in the contralateral SC. Eccentricity representation for each individual SC was measured in separate scanning sessions.

Subjects

For the visual stimulation eccentricity retinotopy experiment, three subjects participated in separate measurements of the two hemifields. Hence, $N = 6$ contralateral SCs were tested for the presence of a retinotopic organization of eccentricity. The same three subjects then participated in the blocked attention experiment. For one subject separate measurements were made for each of the two hemifields, while in the other two subjects one hemifield each was measured (left in subject 2 and right in subject 3); a total of $N = 4$ contralateral SCs. Multiple sessions were collected for hemifields where the data

was too noisy. Subjects performed several two-hour-long scanning sessions: 2—4 visual stimulation retinotopies, and 1—4 blocked visual attention.

Visual stimulus protocols

Eccentricity representation of visual stimulation

Stimulus was a 50° polar angle sector of radially moving black and white dots (4°/s speed) on a mean luminance gray background, which was subdivided into 4 virtual sections (Fig. 9A). The sector had an eccentricity span of 5° and periodically swept across the horizontal meridian at 6 positions with mean radius values of 5°, 10°, 15°, 20°, 25° and 30°. Because the size of the constant polar angle sectors increased with increasing eccentricities, the size of the dots was also scaled up proportionately. The task of the subjects was to discriminate if dots in one of the sections were moving at a speed faster or slower than dots in the other sections, while maintaining fixation. A single trial of moving dots display lasted for 2 sec, and subjects were required to make a response by pressing one of two buttons indicating their judgment of faster or slower, within the last 0.5-sec of the trial period. Subjects were instructed to maintain attention during the display period and be as accurate as possible. There were 2 trials at each position and the radial direction of the dots with respect to fixation alternated between inward and outward after each trial to prevent adaptation. The sector swept across the display spanning the 6 positions for 9.5 cycles with a 24-second period. Task performance of the subjects was maintained at >71% using a staircase procedure similar to the polar angle stimuli.

Before the scanning sessions, subjects practiced the task outside the scanner for 2—3 20-min training sessions until their performance stabilized. The initial speed difference was based upon their performance during these training sessions, and was

typically 0.9—1.5°/s. During fMRI scanning sessions, subjects performed this task over the course of multiple ~4-min-duration runs.

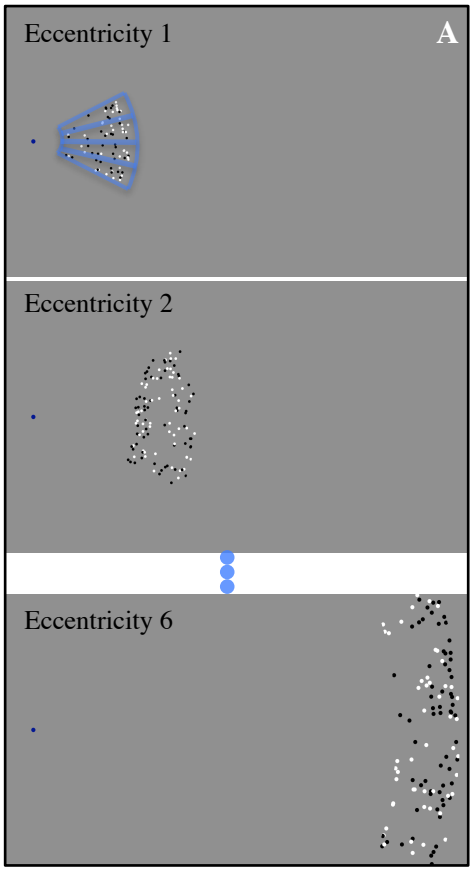

Figure 9: Eccentricity stimuli for stimulation retinotopy and blocked attention. A) For the stimulation experiment, a 50° sector of moving black-and-white dots on a gray background slowly swept away from fixation, which was one edge of the screen. The sector was divided into 4 virtual section (blue lines in figure) to enable the subject to perform a speed discrimination task in a random sector. B) In the visual attention experiment, the stimulus was two sectors of similar moving-dots again divided into 4 virtual sections each, which was always present on the screen. Subjects were cued by the color of the fixation dot to alternate attention between two sectors (orange and green for small and large eccentricity respectively) in 12-sec blocks and perform a similar speed-discrimination task within the cued sector

Eccentricity representation of visual attention

Stimulus was two 50° sectors of moving dots at eccentricities 6—10° and 22—28°, each divided into 4 virtual sections (Fig 9B). Subjects' task was to alternate attention between the two sectors in 12-sec blocks cued by the color of the fixation dot (orange for small and green for large eccentricities) and perform six 2-sec dot speed discrimination trials (same as described for previous stimuli) within the cued sector while trying to ignore the dot-speed change within the other sector. For the last trial of

each block the fixation dot changed to yellow as an indicator that the subjects would need to shift attention at the onset of the next trial. Subjects' performance was adjusted using a similar staircase procedure as described previously.

Image analysis

The image analysis was performed in manner described in Chapter II. The data within the reference volume was averaged over a depth of 0—1.6 or 0—1.8 mm for the visual stimulation retinotopies and 0—1.4 or 0—1.6 mm for blocked attention, depending on what produced a greater amount of activation at a threshold of $p < 0.05$.

Eccentricity representation of visual stimulation

To quantify the eccentricity retinotopy data, regions corresponding to the 50° polar angle width of the stimulus aperture were defined for each subject from the polar angle retinotopic maps. In order to obtain contiguous regions that were contiguous the polar angle phase progression was first fit with a smooth polar angle map, $M(x, y)$. This was done in the following manner.

The depth-averaged polar angle phases for each dataset were transferred onto the respective flattened SC. Then the estimated hemodynamic delay (see Chapter III, Methods) was subtracted from polar angle retinotopy phases to get a 2-D matrix of phases, $P(x, y)$. A least-squared fit was performed to $P(x, y)$ with a bivariate polynomial of the third order, $M(x, y)$, within the independent ROIs obtained from lateralized stimulation sessions (see Chapter III, Methods).

The map to be modeled is given by:

$$M(x,y) = C_0 + C_1.x^3 + C_2.x^2y + C_3.xy^2 + C_4.y^3 + C_5.x^2 + C_6.xy \ldots$$
$$+C_7.y^2 + C_8.x + C_9.y$$

where x and y are the flat map Cartesian coordinates, and C_0, C_1…, C_9 are coefficients that need to be determined for the least-squared fit.

$M(x, y)$ can be written in matrix form as:

$$M(x, y) = X \times C$$

where,

$$C = [C_0 \quad C_1 \quad \dots \quad C_9]$$

and,

$$X(x, y) = \begin{bmatrix} 1 \\ x^3 \\ x^2y \\ xy^2 \\ y^3 \\ x^2 \\ 2xy \\ y^2 \\ x \\ y \end{bmatrix}$$

then for a least-squared fit:

$$X \times C = P$$

$$C = X^{-1}P$$

This fit provided a 2-D spatial gradient map of the polar angle retinotopy for each individual colliculus, which could then be used to delineate regions corresponding to the desired polar angle range. For analyzing the eccentricity data, 50° polar angle regions along the horizontal were defined for each of left and right SC. However, since the eccentricity extent of the polar angle mapping stimulus was only 10°, these regions did not cover the entire rostro-caudal extent of the eccentricity data (corresponding to a 30° stimulus FOV). Therefore, these 10° ROIs were transformed back into the reference volume and overlaid along with the phase data upon the 3D surface representation (Fig.

10, green outlines). Then, based on an initial calculation of the phase gradient direction (procedure described in Chapter II), they were manually extended along the direction of increasing phase progression (Fig. 10, dashed black outlines), which could be discerned by eye in all contralateral SCs.

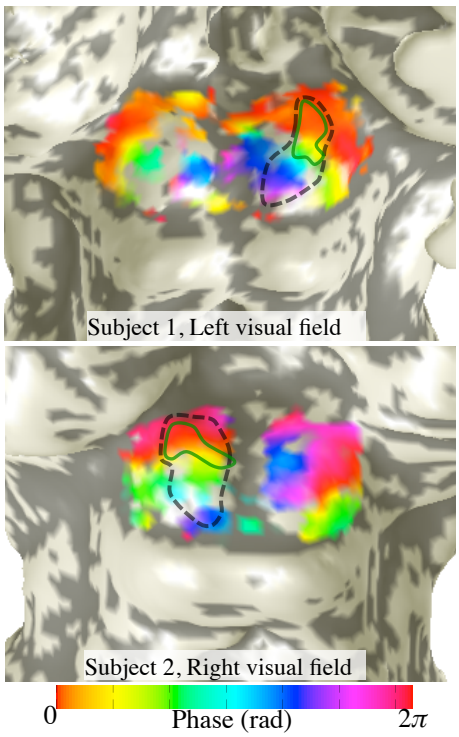

Figure 10: ROI definition to analyze eccentricity retinotopy data in two sample datasets (subject 1, right colliculus and subject 2, left colliculus). Green outlines are ROIs from polar angle retinotopic maps that correspond to 50° along the horizontal. Dashed black outlines are ROIs extended along the phase progression that were used in the eccentricity retinotopy analysis.

Similar fitting procedures as described above were also performed on the eccentricity retinotopy phase data within these eccentricity ROIs, to form smooth eccentricity maps. The hemodynamic delay to be subtracted from the phases prior to the fit was the mean phase of 3—5 of the rostral-most voxels within the ROI (rostral-most voxels determined by eye based on anatomical landmarks from the 3D surface representation). This calculation of the hemodynamic delay was based on the assumption from monkey SC maps that smaller eccentricities, which were presented first in the stimulus, were represented most rostrally. Phase were then normalized on the range 5—30° to give actual eccentricity values. From the smooth eccentricity retinotopy map, ROIs corresponding to the stimulus sectors in the attention experiment could be delineated (Fig. 12).

Eccentricity representation of visual attention

The fitted eccentricity retinotopy map were used to delineate ROIs corresponding to the 6—10° and 22—28° sectors for the blocked attention experiment. In the stimulus paradigm, visual attention was alternated between large and small eccentricity sectors in 12-sec blocks. If attention were topographically organized within SC in a manner similar to stimulation, its expected response to the small and large eccentricity sectors would occur in the rostral and caudal portions of the contralateral SC respectively. Because the stimulus was a block alternation, the fMRI response between the two sectors would be expected to have a phase difference of π radians. Therefore, to test registration between stimulation and attention, the phase difference within the two ROIs was tested. The phase difference was also bootstrapped across runs for each contralateral SC, to provide 68% confidence interval and tested against the null hypothesis that the phase difference was < 0 (after taking into account phase wrapping).

RESULTS

Behavioral performance

All subjects successfully maintained accuracy at >71% during each session. For the stimulation retinotopy and blocked attention experiments the average performance across subjects was 79% and 78% respectively. Mean discrimination thresholds were 0.9°/sec for the stimulation retinotopy and 1.2°/sec for the blocked attention experiment.

Eccentricity representation of visual stimulation

Fig. 11 shows phase data for three subjects for the right and left hemifields (in left and right columns respectively). Colors represent visual field eccentricity with the red-yellow region corresponding to small eccentricities and cyan-blue-magenta corresponding to large eccentricities. The ROIs extended from the polar angle map

predictions are outlined using dark dashed lines for each colliculus. The phase data overlay is thresholded with an alpha blending procedure such that the fully opaque colors are at $p < 0.05$ (p-values calculated using bootstrapping procedure described in Chapter II), while data having $0.05 \leq p < 0.16$ are overlaid with gradually fading transparency. This was done in order to show that the phase progression was continuous despite some regions of data with $p > 0.05$.

Retinotopic organization within the contralateral SCs (left for right visual field and vice-versa) was quantified by calculating the direction and reliability of the phase gradient within the outlined ROIs. Reliability of the phase gradient was statistically significant ($p < 0.03$) in 2/6 colliculi (subjects 2 and 3, right SC) (Table 2). Average data grouped by combining all six colliculi showed a substantial, but was not statistically significant ($p > 0.12$). The black arrows under the respective colliculi indicate the calculated direction of the phase progression along with bootstrapped 68% confidence intervals indicated by the brown arrows within the same ROIs. In both colliculi that had a reliable phase gradient, the progression was from the rostral to caudal direction (Fig. 11).

	Phase gradient p-values	
Subject	Left SC	Right SC
1	0.119	0.124
2	0.356	0.009
3	0.111	0.024
Combined	0.124	

Table 2: *P*-values on the reliability of the eccentricity phase gradient obtained by bootstrapping for individual and combined colliculi.

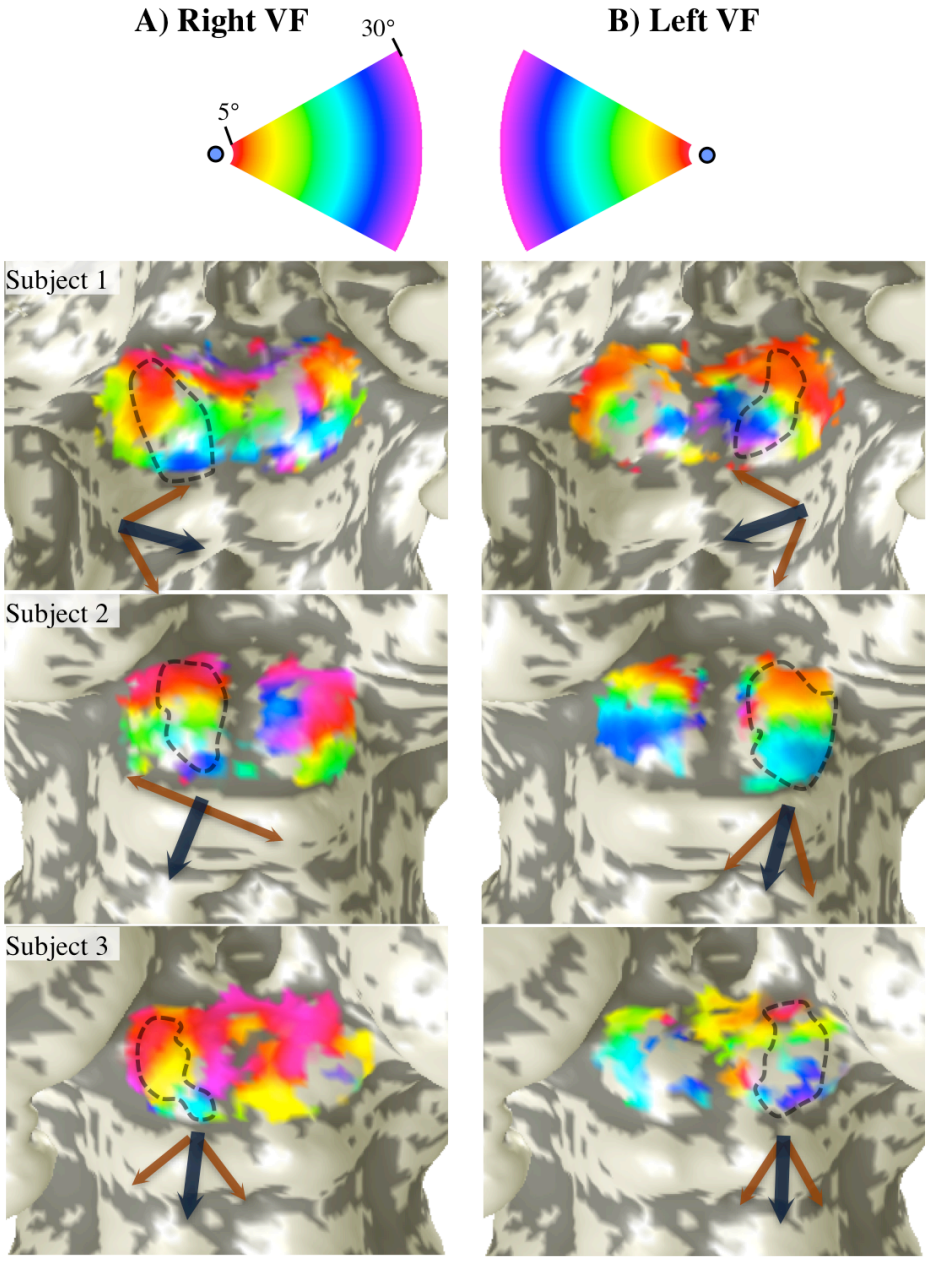

Figure 11: Eccentricity retinotopic maps for visual stimulation in three subjects; *left*: maps for the right visual field (VF), *right*: left VF. Color wedges at the top relate the overlaid phases to their eccentricity; blue dots indicate fixation mark. ROIs for eccentricity retinotopy analysis are indicated black dashed outlines. Arrows under each contralateral SC depict the direction of phase gradient (black arrows), with 68% confidence intervals (brown arrows).

Visual inspection revealed a progression of phases from low to high eccentricities along the rostral to caudal direction in at least 4/6 contralateral colliculi, right SC for subjects 1 and 3, both SCs for subject 2. The phase progression on the right SC for subject 1 had a rostro-lateral to caudo-medial tilt in its orientation. The left SC of subject 1 had a wide spread of low eccentricity responses along the rostral and lateral margins of the colliculus with high eccentricities represented caudally. For subject 2 the right SC phase progression covered only about three-fourths of the entire gamut of phases, indicating that a response for the largest (or smallest) eccentricities was not observed. For subject 3, the left SC had a small-to-medium eccentricity representation from the rostro-lateral to caudo-medial direction near the lateral portions of the colliculus after which the phase progression for high-eccentricities seemed to turn back rostrally along the medial margin of the colliculus.

In some data there was a progression of phases from rostral to caudal direction evident in the ipsilateral colliculus. This was most noticeable in data for both hemifields in subjects 1 & 2. This ipsilateral phase progression typically covered about a half to three-fourths of the complete phase progression and was strongest along the lateral portions of the respective colliculi. For subject 1 the ipsilateral phase progression on both sides occurred outside (lateral to) the regions predicted by the polar-angle map, while for subject 2 it occurred within the polar-angle range on both sides.

The phase progression for each contralateral colliculus was visualized on a flattened representation (Fig. 12A, B), and fit with a third order 2-D polynomial to obtain a smooth eccentricity map (Fig. 12C). These fitted eccentricity maps were used to delineate ROIs corresponding to different stimulus eccentricities to perform eccentricity specific analysis for the attention experiments reported below (Fig. 12C, D).

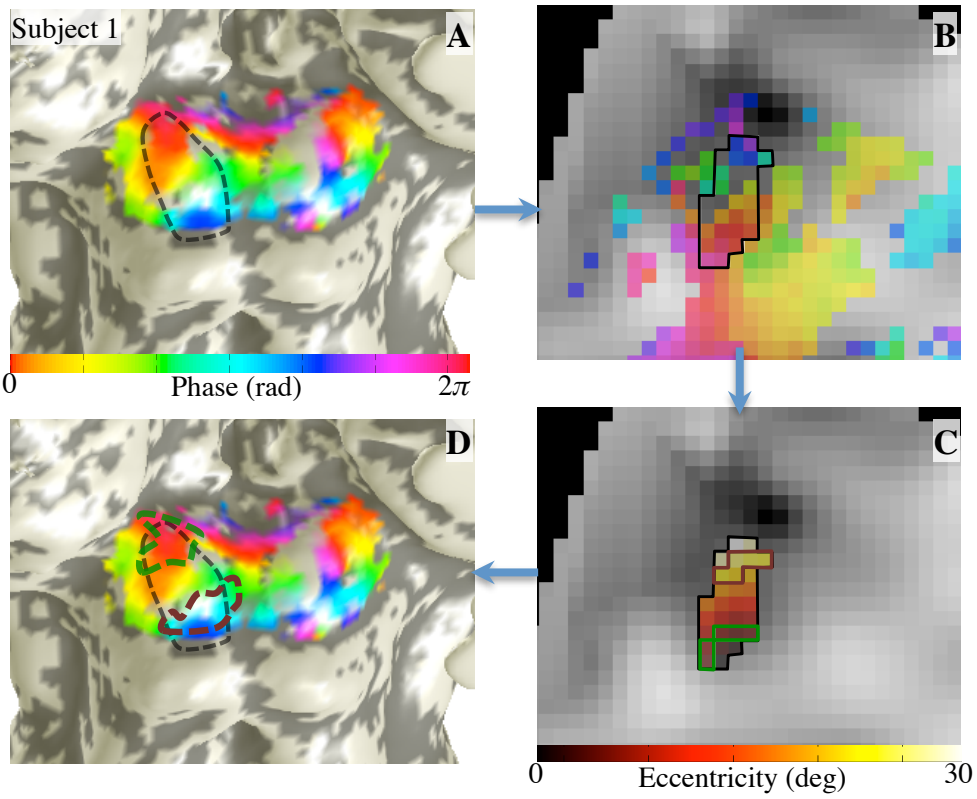

Figure 12: Fitting a smooth map to eccentricity phase progression. A) Eccentricity retinotopy data in subject 1, left colliculus. B) Phase data and ROI overlaid on a flattened representation of that colliculus. C) Fitted eccentricity map with ROIs corresponding to small (green) and large (brown) eccentricities. D) ROIs transformed back onto 3D surface.

Within these stimulation eccentricity maps, the mean surface area of activation across the six colliculi for the inner 10° was 37±11% (mean and standard deviation) of the respective ROIs. For an eccentricity of 15° this value was 56±13%.

Eccentricity representation of visual attention

Fig. 13 shows phase data for the four contralateral colliculi (subject 1: left and right SC, subject 2: left SC, subject 3: right SC; from here on referred to as colliculus 1—4 in that order) for which attention to eccentricity measurements were made. Again the

phase data was overlaid with an alpha blending procedure such that the fully opaque colors are at $p < 0.05$, while data having $0.05 \leq p < 0.06$ are overlaid with fading transparency. Visual inspection indicated that colliculi 1—3 had low-phase activity in the caudal portions of SC and high-phase activity in rostral SC, which was consistent with the order of presentation of the large and small eccentricity sectors respectively.

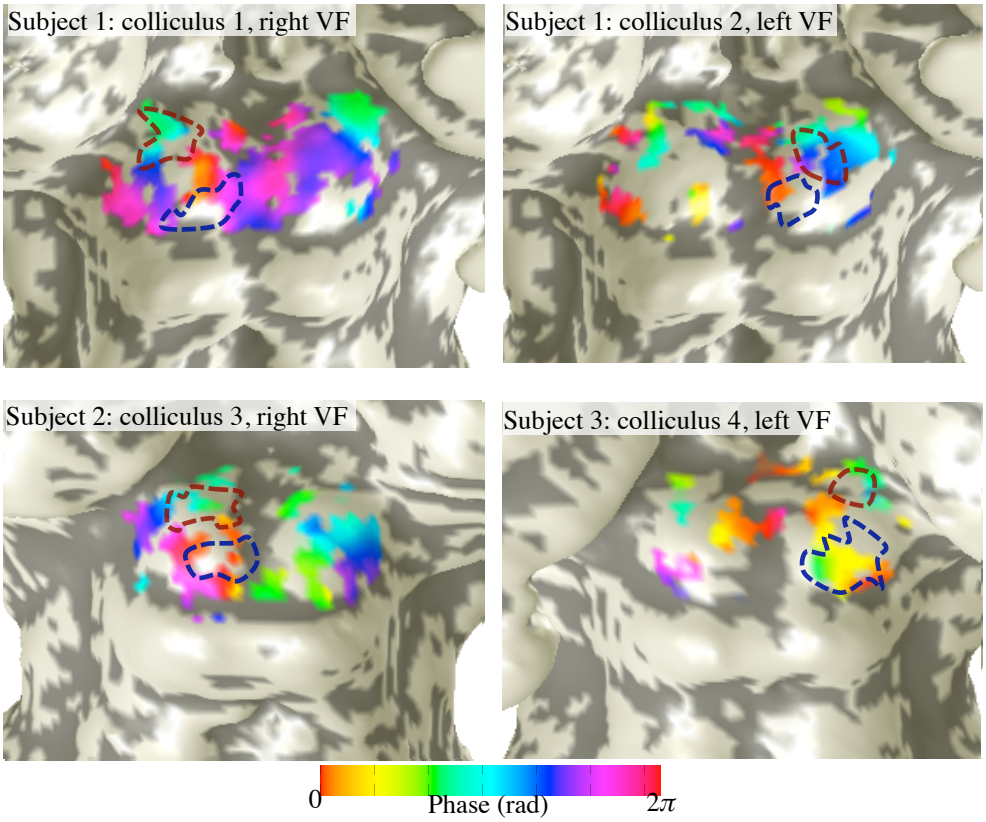

Figure 13: Eccentricity representation of visual attention. Phase data for four sampled contralateral colliculi (subject 1: both SCs, subject 2: left SC, subject 3: right SC) thresholded at $p < 0.05$. Small (maroon) and large (dark blue) eccentricity ROIs from stimulation retinotopies overlaid.

The maroon and dark blue outlines on each colliculus are ROIs corresponding to the small and large eccentricity sectors obtained from the modeled visual stimulation

eccentricity maps. Within these two ROIs, complex amplitudes were bootstrapped to get confidence intervals on the phase differences between the small and large eccentricity ROIs and tested against the null hypothesis that there was no phase difference. Means of the difference of phases for individual and combined colliculi within these ROIs along with 68% confidence intervals are plotted in Fig. 14. The bootstrapped phase difference distributions were significantly >0 at $p < 0.05$ in 3/4 individual and combined colliculi. Overall mean of the phase difference was centered close to π radians (3.06 radians) confirming counter-phase alternation in temporal coincidence with the stimulus alternations within the independently defined small and large eccentricity ROIs.

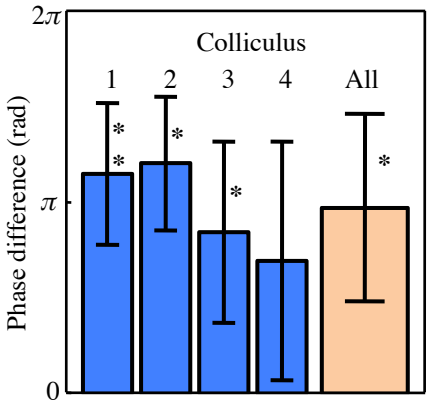

Figure 14: Phase difference between the large and small eccentricity ROIs for four individual and combined colliculi (Asterisks denote significance: $**p < 0.005$, $*p < 0.05$).

Looking at the spatial pattern of activity for the attention data (Fig. 13) it seemed that the ROIs corresponding to the large eccentricity sectors were misaligned with the regions of strongest low phase activity in caudal portion of SC. Therefore, another analysis was conducted to quantify the amplitudes and localization error of the responses. For each blocked attention dataset a reference region (2—3 voxels in the reference volume) was defined based on the overlap of the small eccentricity ROI with rostral SC activation at a coherence threshold >0.20. The phase of this reference region was used to create univariate amplitudes for the entire data as well as to bootstrap the univariate amplitudes across runs (see Chapter II, Image analysis). Because both positive and negative halves of the univariate amplitudes were evaluated for significance a two-tailed distribution comparison was used.

Significant amplitudes at $p < 0.05$ ($p < 0.025$ at the negative and positive halves) for each colliculus are shown in Fig. 15. The small and large eccentricity ROIs from the retinotopy are rendered with partial transparency so they don't interfere with data visualization while still permitting comparison of the spatial localization of maximum amplitudes with respect to the ROIs. Colliculi 1 through 3 showed significant fMRI amplitudes that by eye seemed consistent with the direction of the stimulation eccentricity maps shown in Fig. 11. In colliculus 2, positive (in-phase) and negative (out-of-phase) amplitudes were observed in the rostral and the caudal SC respectively, somewhat laterally to the large eccentricity ROI. For colliculi 1 and 2 the activation pattern had a substantial rostro-lateral to caudo-medial tilt in the orientation that seemed consistent with the measured angle of retinotopy in those colliculi (see Fig 11), with the data occurring more rostro-medially to the ROI in both. Colliculus 2 also had some out-of-phase activation near the rostral pole of the SC that did not correspond to the expected retinotopic location of the large eccentricity response. It is possible that this activation was a vascular artifact and/or corresponds to fixation related neural activity during the large eccentricity attention blocks. Finally, colliculus 4 did not show the expected rostral-caudal pattern for positive and negative amplitudes respectively at $p < 0.05$.

In the three colliculi that showed a significant positive and negative response (colliculi 1, 2 and 3) the rostral ROIs coincided with the activity, which would be expected since the reference phase was calculated from these ROIs. To characterize the spatial misalignment for the large eccentricity response, spatial centroids were calculated for the blue outlined ROIs and the voxels responsive at $p < 0.05$ (cyan/blue voxels in Fig. 15). The centroid differences were 1.6, 1.5 and 1.9 mm for colliculi 1, 2 and 3 respectively.

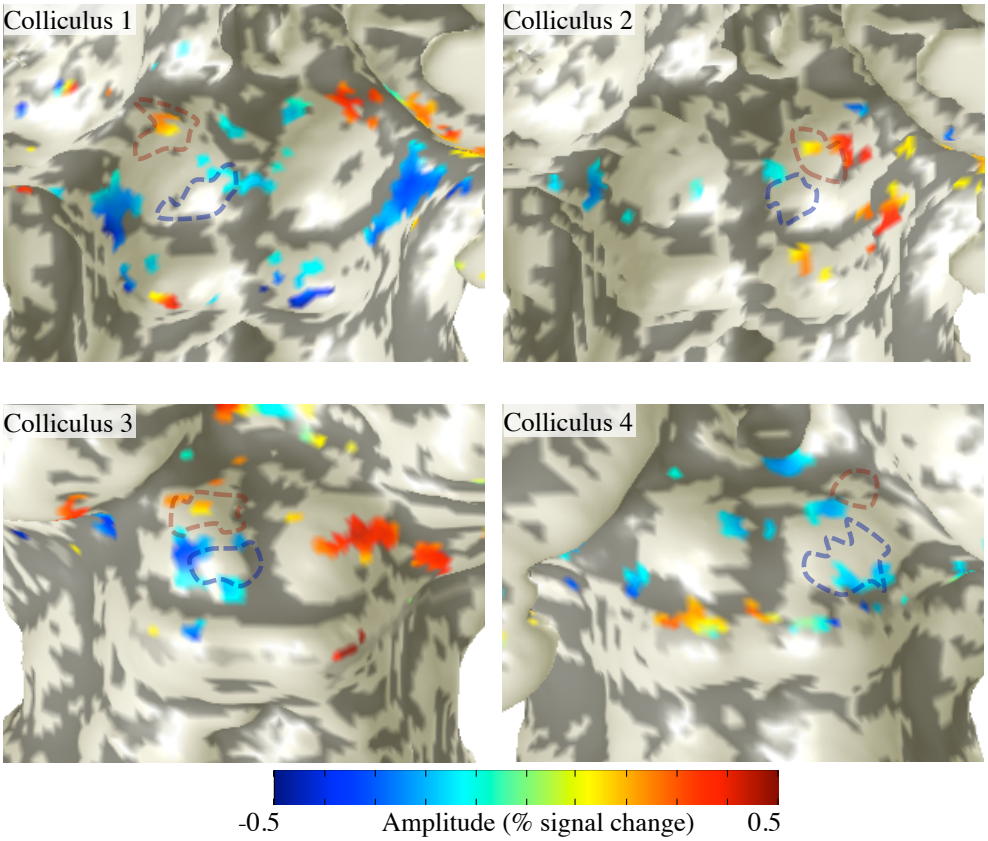

Figure 15: Amplitudes data for eccentricity of visual attention. Univariate amplitudes thresholded at $p < 0.05$ in the four sampled contralateral colliculi. Small and large eccentricity ROIs overlaid with translucence to permit visualization of underlying data.

DISCUSSION

There was a topographic progression of signals evoked by visual stimulation for eccentricity along the rostral to caudal direction in 2/6 contralateral SCs. Visual inspection, however, did indicate a progression of phases along the rostral-caudal direction in at least two other SCs (subject 1: right, subject 2: left; Fig. 11), which did not have a statistically significant phase gradient. Phase gradient data combined over all colliculi also did not show a statistically significant effect. This lack of reliability reflected the overall low SNR of the eccentricity measurements in general. In some

colliculi there was a tilt in the phase progression such that the rostral representation shifted laterally and the caudal representation medially (subject 1: bilateral, subject 3: left). Notwithstanding the weak SNR, the representation of eccentricity in human SC was found to be consistent in orientation with visual stimulation response along eccentricity in non-human primates (Cynader and Berman, 1972; Goldberg and Wurtz, 1972a). Visual attention also had a topographic organization, with response for smaller eccentricities located rostro-laterally and larger eccentricities located caudo-medially within 3/4 contralateral SCs. The location of the visual attention signals was consistent within a mean spatial error of ~1.7 mm to the location predicted by the retinotopic map of eccentricity for visual stimulation.

A previous study was unable to find the representation of eccentricity signals within human SC (Schneider and Kastner, 2005). Some potential reasons for their inability to measure these signals have been outlined earlier. While most of the reasons could have been partly responsible for their negative findings, the results presented here indicate the importance of the spatial resolution within the portion of the colliculus corresponding to the stimulus FOV. At eccentricities of 15° (used in their experiments) just over half the SC maps shown here are activated. This comes to an average of about 25 voxels across the SC surface at the current resolution of 1.2 mm, which implies 5-7 voxels to show a phase progression along any particular direction. At their resolutions this would come to about 3-5 voxels to discern the eccentricity map. Thus, their coarser sampling may have reduced the reliability of their eccentricity mapping data.

Overall, the sinusoidal coherence model obtained for the eccentricity data was much less reliable than polar angle maps shown in Chapter III. One reason for this may have to do with variable BOLD response sensitivity over the surface of the SC and non-uniformity in such sensitivity between the medial-lateral versus the rostral-caudal axes.

The data suggests that the reliability is best at the rostral edge of the SC, worsening around the middle and again improving towards at caudal edge of the SC. A perfusion experiment would be necessary to investigate this hypothesis. Alternatively or additionally, this could be due to an increasing difficulty of subjects to attend to large eccentricities compared to the iso-eccentric stimulus for polar angle. Because the use of the staircase precludes testing this hypothesis using the existing within-scanner behavioral data, we conducted psychophysics in two subjects without using a staircase indicated that this was indeed the case, with performance declining steeply for the two outermost eccentricities in particular (Fig. 16).

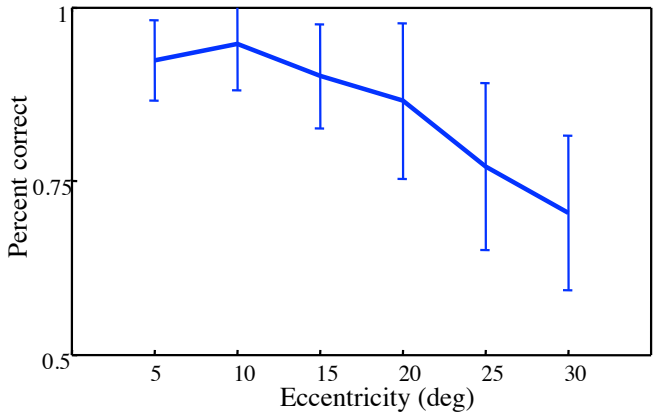

Figure 16: Percent correct performance vs. eccentricity plot. Average over two subjects. Error bars are standard errors of the means.

As these experiments were conducted using a single hemifield stimuli, the response was expected to occur in the SC contralateral to the stimulated visual field. However, in at least 4/6 colliculi there was also a rostral to caudal phase progression for visual stimulation within the ipsilateral colliculus. This finding was unexpected based on the non-human primate literature. There could be a few non-exclusive possible reasons for this ipsilateral phase progression. First, this could be a purely vascular artifact. This could happen if there was a common sink of vascular drainage from both colliculi, oriented in a rostral to caudal manner. A vascular artifact explanation was also supported by noting that the ipsilateral progression was most prominent along the lateral groove of the colliculus, which may have a tendency to have a

higher concentration of bigger vessels including draining veins. A susceptibility or "venography" experiment would provide more insight into this hypothesis. Second, it is known that the SC contains a retinotopic map of eye movements aligned with the map of visual stimulation. Because eyes were not tracked during the scanning sessions, it is possible that the subjects were making infrequent saccadic eye movements to the stimulus sector and back to the fixation spot. In such a scenario, the ipsiversive saccades could potentially induce retinotopic activity within the ipsilateral colliculus. Moreover, for these experiments a single hemifield stimulus was used and subjects were required to rotate their head toward the edge of the screen. Subjects often reported that during scanning procedures the fixation spot was visible only to one eye, with the birdcage head coil blocking the fixation spot from the other eye. Subjects had not practiced the task outside the scanner with such a scenario, and therefore, could have made eye-movements in the scanner, even while being good fixators under regular conditions. Eye tracking experiments conducted with reproduction of the scenario of one-eyed fixation while performing the eccentricity task may provide more insight into their behavior and therefore the responses. Third, based on the currently knowledge of the origins of the BOLD response, it is unclear if the fMRI signal is able to distinguish between inhibitory and excitatory neuronal activity. The ipsilateral phase progression could be due to the neuronal activity of the ipsilateral inhibitory neurons receiving retinotopically organized suppressive signals from the contralateral SC. Such a mutual inhibition of responses between colliculi is believed to be the cause of the 'Sprague effect' in cat SC, where hemianopia observed after removal of the contralateral visual cortex is partly relieved by the subsequent removal of the ipsilateral SC or splitting of the collicular commissure (Sprague, 1966). Fourth, since this is the first time any such measurements are being made in humans, it is possible, that there is an ipsilateral representation of visual

stimulation in human SC. Finally, even if there isn't an ipsilateral representation of visual stimulation, since the experiment involved an active behavioral task within the stimulus aperture, it is possible that SC has an ipsilateral topographic representation of visual attention. Such an ipsilateral representation of attention has also been reported recently in higher visual areas (Brefczynski-Lewis et al., 2009).

Overall, the visual stimulation eccentricity measurements presented here and their spatial precision with the attention signals indicate the reliability of the MRI methods used for the functional neuroimaging of the SC in this dissertation. Having established the presence of a complete retinotopic organization of visual stimulation signals in human SC enables us to perform vision science experiments with a fair degree of spatial precision. The next chapter explores a set of such experiments investigating in greater detail the nature of visual attention signals in human SC.

Chapter V: Base response – threshold contrast-detection signals in SC

Recent work demonstrating that manipulation of SC activity in non-human primates directly affects behavior during covert attention tasks has suggested a critical role for the SC in visual attention (Cavanaugh et al., 2006; Cavanaugh and Wurtz, 2004; Lovejoy and Krauzlis, 2009; Muller et al., 2005; Zenon and Krauzlis, 2012). Studies in both primates (Ignashchenkova et al., 2004; Wurtz and Mohler, 1976) and humans (Katyal et al., 2010; Schneider and Kastner, 2009) show a retinotopically specific enhancement of SC activity when covert attention is deployed upon a supra-threshold visual stimulus.

In primate cortex, visual areas also respond to covert attention (Kastner and Ungerleider, 2000; Maunsell and Treue, 2006; Reynolds and Chelazzi, 2004). Strong attention effects have been observed in human early visual cortex even in the absence of visual stimulation (Kastner et al., 1999). In particular, there is a boost in fMRI activity in early visual cortex during threshold-contrast detection, an attentional "base response" (Ress et al., 2000; Silver et al., 2007). High-resolution fMRI was used to investigate if SC exhibits a similar base response.

Electrophysiology studies in macaque SC show that correlates of attention are observed in both superficial-layer visually responsive and intermediate-layer visuomotor neurons (Cavanaugh et al., 2006; Ignashchenkova et al., 2004; Wurtz and Mohler, 1976). Specifically, the activity of visually responsive neurons is enhanced only for the duration of stimulus presentation, while visuomotor neurons also exhibit a delay period baseline response enhancement between cue offset and stimulus onset (Ignashchenkova et al., 2004; Wurtz and Goldberg, 1972). The delay-period visuomotor activity has been

proposed to be a correlate of the oculomotor theory of attention (Moore et al., 2003; Rizzolatti et al., 1987).

In the experiments presented in Chapter III it was shown that covert attention toward a strong visual stimulus boosted responses close to the superficial SC surface. This could have corresponded to an enhancement of only the superficial-layer visual neurons or both visual and intermediate-layer visuomotor neurons; the measurements were not able to resolve this fine-grained distinction.

This study investigates the presence of a base response in SC during threshold-contrast detection, and if present examine its depth profile. By greatly reducing and counterbalancing the exogenous stimulus drive, the attention signals are expected to be of a sustained endogenous nature. Moreover, if attention were mediated by the intermediate-layer neurons, then by diminishing the sensory response of the superficial-layer visual neurons, base response would be expected to occur more deeply within SC tissue than the response evoked by attention directed toward a high-contrast stimulus.

METHODS

Subjects

Five subjects participated in 2—4 2-hr-long scanning sessions: one localizer to characterize the representation of the stimulus aperture and 1—3 attentional base response sessions. Three subjects participated in the control experiment. For two of the five subjects attention with high-contrast stimulation data was used from the lateralized attention experiment described in Chapter III, while the other three subjects participated in scanning sessions for the same stimulus for this experiment separately.

Visual stimulus methods

All experiments used the large-screen LCD TV display (#1, see General Methods), except for two sessions where an equipment problem necessitated the use of the back-projection display (#2).

Base response

Two black-outlined 45°-width sectors were located along the horizontal meridian to the left and right of the central fixation dot at eccentricity 4—7.5° (Fig. 17A). Subjects alternated attention between the two sectors in 12-sec blocks. Each alternation began with a 2-sec duration fixation dot color-change cue to attend the left sector (Fig. 17C). For the remainder of the block, a small arrow below fixation indicated the attended sector. The remaining 10 sec contained four trials. For the first 2 sec of each trial there was a 50% probability of occurrence of a pair of small (0.25° 2σ diameter) briefly presented (~100 ms) Gabors at a random time and location, independently in both sectors (Fig. 17B). At the end of the 2-sec stimulus period, the fixation dot turned yellow, cueing the subject to indicate their judgment about the presence or absence of the Gabors in the attended sector by pressing a button. After four trials on the left side, the fixation changed color for two seconds, cueing subjects to attend to the right sector, where they then performed the same task. This attentional alternation proceeded for 19 blocks, creating runs lasting 228 sec.

Before scanning, subjects performed multiple psychophysics sessions in a side-lab, where the contrast of Gabor patches was continually varied to determine each subject's stable contrast-detection threshold (corresponding to a performance of ~68% correct). Threshold values of the luminance-contrast for these small Gabor varied between 4.5—11% across subjects. For two experimental sessions, display #1 was used. Separate contrast thresholds were obtained using this back-projected stimulus within the scanner bore. The measured threshold contrast value for these two sessions was

substantially higher (16% compared to 6.5% for the LCD), reflecting the display's lower contrast performance.

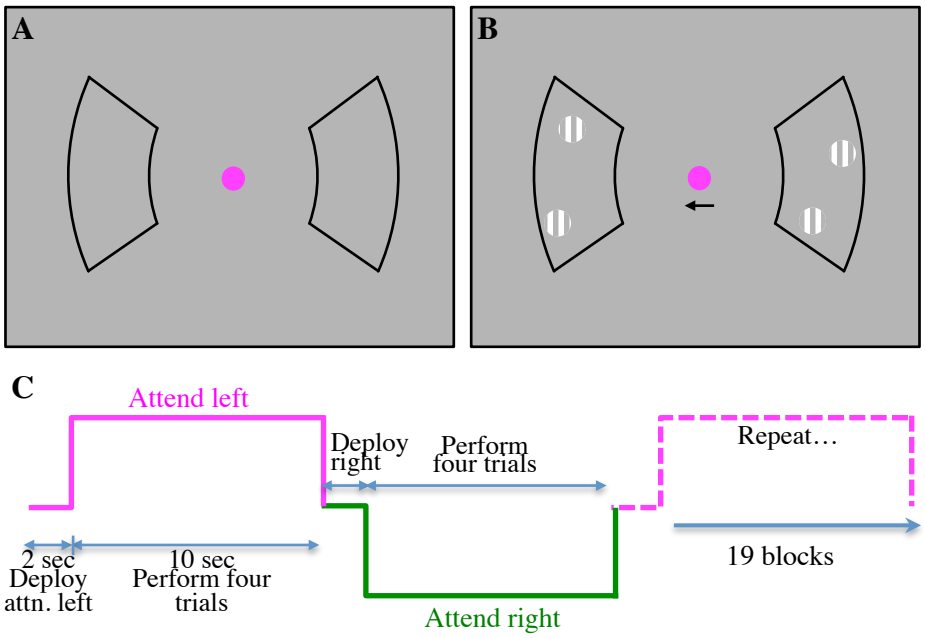

Figure 17: Stimulus and task: A) Blank sectors. B) Sectors with Gabor detection targets. C) Attention was block-alternated between left (magenta) and right (green) sectors. Blocks began with a 2-sec delay to deploy attention upon the cued sector, and then subjects performed four 2.5-sec trials. During each trial there was a 50% probability that two threshold-contrast Gabors would be presented briefly at a random time and location within each sector. At the end of each trial, subjects pressed a button to indicate their yes/no detection judgment within the cued sector.

Localizer

A sector of moving dots (4°/s speed) was presented at the same aperture as the base-response stimulus in 12-sec alternating blocks on the left and right sides respectively. The sector was sub-divided into 2 × 2 virtual sections, and during each 2-sec trial, dots in one section moved faster or slower than all other sections. Subjects' task was to fixate while discriminating dot speed, and then indicate their judgment by pressing

a button at the end of the trial. There were 19 alternations of the moving-dot stimulus. Task performance of the subjects was maintained at ~71% by adjusting the magnitude of the speed difference between dots using a pair of randomly interleaved two-up-one-down staircases.

Attention with visual stimulation

This was same stimulus described in Chapter III under "Lateralized stimulation and attention". Two sectors of moving dots (4°/s speed) were presented along the left and right horizontal meridians (eccentricity 2—11°, polar angle 144°) simultaneously (Fig. 5). The sectors were divided into 2 × 4 virtual sections, and the task of the subjects was, once again, to discriminate if the dots in one of the sections were moving faster or slower than dots in other sectors. A small arrow below the fixation dot cued subjects to alternate their attention between the left and right sectors in 12-sec blocks. Trials had a 2-sec duration with subjects responding within the last 0.5 sec. Performance was again maintained with the staircase procedure described above.

Control

Stimulus was similar to the base response experiment with two black-outlined sectors (45° polar angle, 4—7.5° eccentricity) along the horizontal meridian on each side of the fixation dot. Instead of the presentation of Gabor stimuli being counter-balanced within the two sectors for each block, Gabors were presented in a 12-sec blocked-alternation between the left and right sectors to maximize any possible fMRI response contrast evoked by the faint stimuli. The presentation frequency, duration and contrast of the Gabors were matched with the base-response experiment for each subject. There were 19 blocks of stimulus alternation. Attention was directed away from the stimulus apertures by having the subjects perform a demanding task at fixation. Fixation dot

changed colors rapidly (every 300 ms) and subjects were required to respond by pressing a button every time the color became green. There was a 2-sec response window after the fixation dot became green within which subjects could make this response.

Image analysis

The image analysis was performed in manner described in Chapter II. The data for the localizer sessions was depth-averaged over a range of 0—1.8, for the base response and control sessions over 0.5—2.2 and for the attention with stimulation sessions over 0—1.6 mm. For visualization base response data was thresholded by *p*-values calculated by bootstrapping the coherence model (described in Chapter II).

ROI definition

From the localizer sessions for each subject, ROIs were delineated by thresholding the data using coherence values to get the strongest 12—15 responsive voxels within the reference volume. All analyses for the base-response, control, and attention with visual stimulation experiments were performed within these independently localized ROIs.

Response amplitude calculation

Univariate amplitudes were calculated as described in Chapter II, by projecting the complex vector within each ROI upon the mean phase vector within that ROI. Therefore, reference phase was defined for each SC separately but based upon the independently localized ROIs. Bootstrapping was performed in a manner similar to that described in Chapter II to obtain confidence intervals.

Depth profile analysis

Depth profiles were plotted for the base-response and attention with stimulation experiments in the manner described in Chapter II. The distance from SC surface of the maximum amplitude of the profiles was calculated over a depth-range of 0—2.5 mm as a measure of the depth of the peak response. Confidence intervals for the peak locations were obtained by bootstrapping the profiles across runs for 10,000 iterations.

RESULTS

Inside the scanner, subjects performed the localizer, base-response, control and attention with visual stimulation experiments while high-resolution fMRI data was obtained.

Behavioral performance

Subjects reported difficulty in detection of the faint Gabor patches in the base-response task but were still able to maintain greater than chance performance during all scanning sessions. The average behavioral performance across subjects for the base-response scanning sessions was 69%.

Base-response experiment

The base-response experiment produced significant ($p < 0.003$) response amplitudes in the ROIs of 9/10 colliculi of the five subjects and for all colliculi combined ($p < 10^{-4}$) (Fig. 18A). The location of activity on the SC surface (Fig. 19) corresponded well to the expected retinotopic locations (black outline ROIs) in the same nine colliculi. In the remaining colliculus (Subject 5, left), there was a substantial trend for localized activity ($p < 0.052$).

Since SC responses are known to be primarily contralateral, the blocked alternation would be expected to produce a 12-sec time delay between the responses of

the two colliculi. Mean delay across subjects was 10.0 sec (68% confidence intervals 7.2—13.5 sec; Fig. 19). The roughly counter-phase character of the lateralized responses supports their correspondence to the cue alternation.

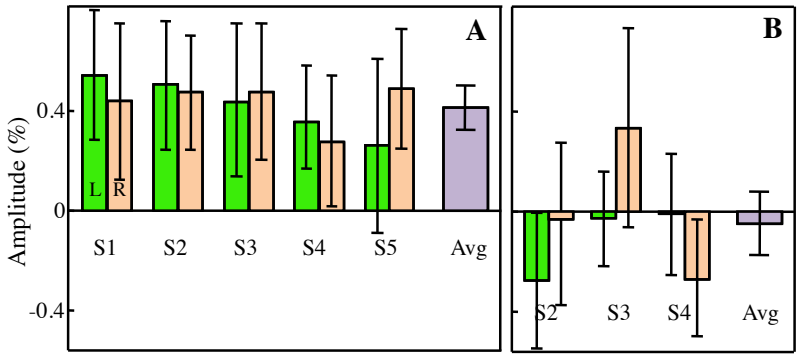

Figure 18: A) Base-response amplitudes in separate colliculi of five subjects and all colliculi combined (error bars are 95% confidence intervals obtained by bootstrapping). B) Control experiment amplitudes.

In subject 4, the base-response session was repeated to measure the repeatability of the spatial location of activation and inter-collicular time delay. The data reproduced at very similar spatial locations (distance between the spatial centroids of activity between sessions: left colliculus, 0.90 mm; right, 0.46 mm) and similar delay (time-delay difference between sessions = 0.42 sec).

Control experiment

Three of the five subjects performed a control experiment to test if the threshold-contrast Gabor detection targets evoked a measureable visual response within the localized SC ROIs. Control experiment amplitudes were not significantly >0 in 5/6 colliculi ($p > 0.52$) and for all colliculi combined ($p > 0.77$, Fig. 18B). Base-response amplitudes were significantly greater than control experiment amplitudes in the same 5/6 colliculi ($p < 0.008$).

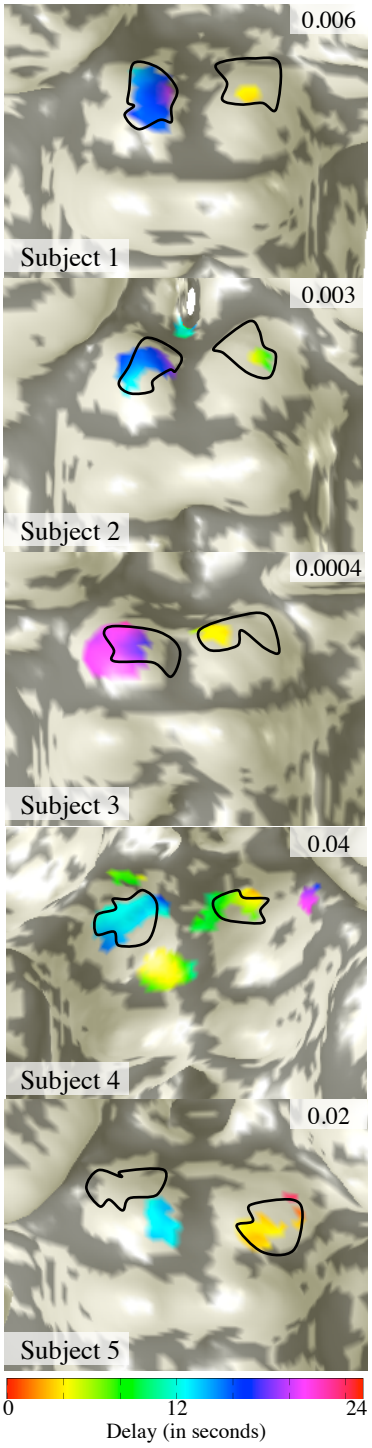

Figure 19: Significant base-response shown on each subject's colliculi with *p*-value thresholds (upper-right); black outlines show retinotopic ROIs. Colors show time-delay of response.

Attention with visual stimulation

This experiment was the same as the one reported in Chapter III, with two of the same subjects. Response amplitudes were significantly >0 in 8/10 individual colliculi ($p < 0.035$) and for all colliculi combined ($p < 10^{-4}$). The data was well lateralized across subjects with a mean delay between colliculi of 12.0 sec (68% confidence intervals 8.7—15.3 sec).

Depth profiles of activity

Fig. 20A shows a plot of the amplitude of fMRI activity vs. depth in the left colliculus of subject 1 for two conditions: base response (blue), and attention with visual stimulation (red). Depth is defined as the distance (in mm) from the interface of cerebrospinal fluid (CSF) and SC tissue (gray vertical line at depth 0 mm). Dotted lines show 68% confidence intervals calculated by bootstrapping. This single colliculus profile shows that attention with stimulation is closer to the SC surface than base response. Fig. 20B shows the averaged depth profiles over all subjects. The profiles show a clear separation in depth, with the peak of the base

response occurring significantly deeper (difference of peaks: 0.63 mm) than the response evoked by attention with stimulation ($p < 0.003$).

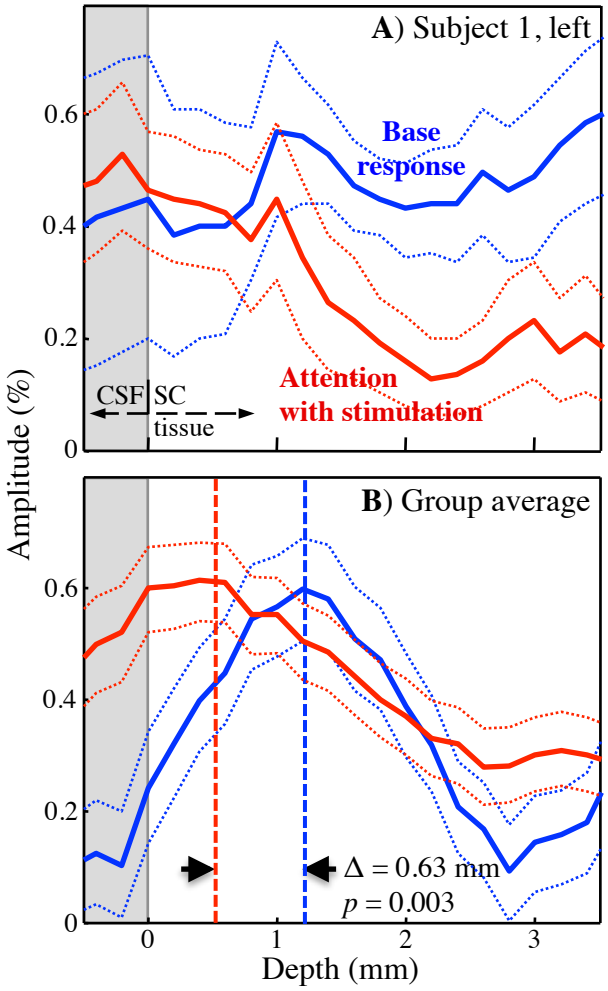

Figure 20: Depth profiles. A) Amplitude vs. depth for base response (blue) and attention with stimulation (red) in subject 1. Dotted lines are 68% confidence intervals. B) Profiles averaged over both colliculi of all subjects.

Eye Movements

All five subjects were experienced psychophysics observers; all but one had >50 hours of experience performing tasks involving maintenance of fixation. To assure that subjects could perform this task while being able to maintain fixation, eye-movements were tracked outside the scanner in three subjects as they performed the base-response paradigm over six 228-sec runs. Saccades were defined as deviations from fixation with speed >250°/sec. Subjects generally held fixation, but did make infrequent (5.8/min) saccades (mean length, 3.8° of visual angle), typically oriented along the vertical direction (mean angle from upper vertical meridian, 1.1°), which were not relevant to our horizontal stimulus paradigm. Hence, saccadic eye movements were not a likely candidate for the observed retinotopically organized base-response activity.

DISCUSSION

Our data show that SC has a retinotopically selective attentional base response, a correlate of sustained endogenous attention, in 9/10 individual colliculi. The base response paradigm used here sought to minimize all exogenous attentional cues by utilizing threshold-contrast stimuli, and counterbalancing their appearance across the two hemifields. Control experiments confirmed that there was insignificant bottom-up response driven by the stimulus itself. Thus, it can be concluded that the observed responses were dominated by sustained endogenous attention.

The base response is temporally correlated with the lateralized task alternation. However, there is some variability in the inter-collicular delay across subjects (7.2—13.5 sec). Such variability could reflect at least three mechanisms. First, subjects may exhibit differences in their ability to deploy attention between the two hemifields. On one side or the other, they may be able to more efficiently deploy their attention during each block. Second, attention may include an ipsilateral response component that is not symmetric between the hemifield representations within the colliculi. Third, the effect could be vascular, corresponding to differences in hemodynamic delays between the two colliculi.

The base-response activity peaks deeper within the depth of the colliculus (~1.2 mm), as compared to a more superficial peak for attentional response to high-contrast visual stimulation (~0.57 mm). Based upon anatomical and neurophysiological studies in primates, these differences are proposed to correspond to the laminar distribution of neuronal subtypes within SC (Ignashchenkova et al., 2004; Wurtz and Mohler, 1976). I propose that the more superficial response for attention with stimulation would correspond to an enhanced activity of both the superficial-layer visual and intermediate-layer visuomotor neurons, while the deeper base response corresponds primarily to the activity of the visuomotor neurons.

This work complements recent studies in macaques that suggest a critical role for SC in endogenous attention. Reversible inactivation of SC in macaques induces behavioral deficits similar to those observed in human attentional neglect (Lovejoy and Krauzlis, 2009; Zenon and Krauzlis, 2012). Also, sub-threshold microstimulation of intermediate layer SC neurons improves behavioral performance in a spatially selective manner that is similar to endogenous attention (Cavanaugh et al., 2006; Muller et al., 2005). However, the same study that observed a baseline increase in visuomotor neuronal activity for attention, showed that it occurred specifically for peripheral and not central cues, suggesting that single-unit enhancement in SC corresponds to exogenous and not endogenous attention (Ignashchenkova et al., 2004).

The contrary finding to single-unit monkey electrophysiology with regards to endogenous attention is similar to the mismatch between results from monkey electrophysiology and human fMRI for baseline enhancement within V1 (Kastner et al., 1999; Lu et al., 2004; Luck et al., 1997). It is possible that effects of endogenous attention upon visuomotor neurons are weak and, therefore, evident only to a population-averaged metric such as fMRI. FMRI responses are known to be correlated more with local field potentials changes, reflecting sub-threshold changes in network inputs, than with the spikes typically measured in single-unit electrophysiology (Logothetis et al., 2001; Logothetis and Wandell, 2004). Alternatively, the fMRI base-response in SC may reflect other subtler variations of the neural dynamics rather than increased firing rate, such as, reduction of spike-rate variability (Mitchell et al., 2007) and/or inter-neuronal correlations (Cohen and Maunsell, 2009).

These results, taken together with monkey electrophysiology results (Cavanaugh and Wurtz, 2004; Ignashchenkova et al., 2004; Kustov and Robinson, 1996; Muller et al.,

2005), provide support for the role of SC in the oculomotor theory of attention in humans (Corbetta et al., 1998; Moore et al., 2003; Rizzolatti et al., 1987).

In monkey SC two classes of saccade-related intermediate layer neurons have been distinguished: "buildup" neurons that exhibit a gradual increase of activity before saccades, and "burst" neurons that fire at saccade onset (Munoz and Wurtz, 1995a). For overt orienting behavior, these two types of neurons operate together to induce saccadic eye movements and head movements (Freedman and Sparks, 1997; Munoz and Wurtz, 1995b; Walton et al., 2007). Recent work in monkeys has shown that this eye-movement generation signal is also projected back upstream from SC intermediate layers to cortex as a corollary discharge (Sommer and Wurtz, 2002, 2004).

The visuomotor neurons showing baseline response enhancement for attention have properties similar to the buildup neurons but for covert attention (Ignashchenkova et al., 2004; Munoz and Wurtz, 1995a; Wurtz and Goldberg, 1972). We speculate that these neurons would accumulate evidence for orienting spatial attention in SC by combining cognitive and multisensory inputs (Sommer and Wurtz, 2000; Wallace et al., 1996). If spatial attention is indeed closely tied to eye movements then SC seems to be well situated within the oculomotor hierarchy to also project these signals back upstream to modulate cortex. This would implicate SC in being a part of a subcortical branch of the top-down attention network, in addition to the more generally accepted fronto-parietal cortical network (Corbetta, 1998; Corbetta and Shulman, 2002). Such a network of attention has also been previously speculated (Kastner and Pinsk, 2004), where putative covert attention signals from SC may be conveyed to the dorsal visual stream by way of the dorso-medial nucleus of the pulvinar (Pdm) in the thalamus (Kastner et al., 2004). Some published work suggests that intermediate layers of SC project to the Pdm, which

in turn is known to be modulated by visual attention and project to posterior parietal cortex (Grieve et al., 2000; Robinson and Petersen, 1992).

However, a recent macaque study has demonstrated that the behavioral deficit in attention caused by reversibly deactivating the SC is not reflected at the neuronal level in visual areas MT and MST (Zenon and Krauzlis, 2012) providing argument against the direct influence of SC upon attention signals in early visual cortex. The same study confirms that SC inactivation nevertheless causes attentional behavioral deficits, suggesting that SC attentional signals may be acting through an alternate portion of the visual stream, possibly visual thalamus (Haynes et al., 2005; Kastner et al., 2004; McAlonan et al., 2008; O'Connor et al., 2002; Smith et al., 2009).

Chapter VI: Conclusions

Superior colliculus is an extensively studied region of the brain in non-human primates and has been shown to play a critical role in sensory-to-gaze transformation and more recently, in visual attention. However, thus far its investigation in humans has been limited owing to methodological challenges faced while performing noninvasive functional imaging of the SC. Work presented in this dissertation uses a novel collection of MRI methods that is able to overcome some of the challenges associated with imaging the SC and demonstrates a fine-scale characterization of visual stimulation and attention signals in human SC. Here I summarize the methods and findings presented in this dissertation and their broader implications. While I played a significant role in the development of all these methods, they were developed by the collaborative work of several people in our lab.

Due to their small size and proximity to large blood vessels, fMRI responses in brainstem structures operate in a relatively low functional SNR regime. An interleaved (3-shot) spiral sequence provided a useful means of physiological noise suppression by filtering out pulsatile noise, which can frequently become aliased at the stimulus repetition frequency. Measurement of the T_2^* value of SC tissue (~65 ms compared to ~48 ms in visual cortex), and proportional adjustment of the echo time, T_E, enabled the acquisition of fMRI signal when its BOLD contrast was maximal, improving the data quality. FMRI data was collected at a spatial resolution of 1.2 mm isovoxels, a factor of ~2.6 higher compared the similar previous studies of SC (Linzenbold and Himmelbach, 2012; Schneider and Kastner, 2005, 2009). Although the use of smaller voxel size reduces the raw SNR, when operating in small subcortical nuclei, it is critical to use smaller voxel sizes. Smaller voxels prevent partial volume effects, i.e., “bleeding” of

response from large neighboring blood vessels. In fact, even at the current spatial resolution partial volume effects were probably not eliminated entirely. The drawback of using high-resolution in terms of SNR was at least partially mitigated by the use of complementary post processing averaging procedures.

For data with low SNR (typical for the attention experiments in SC) multiple session repeats of the same experiment were averaged with the help of a structural reference volume. This reference volume was collected separately at a high-resolution (0.6 or 0.7 mm isovoxels). Within this reference volume tissue-CSF boundary of the midbrain was segmented to form surface models of tissue. These surface models had a trifold advantage (Ress et al., 2007). First, they permitted analysis of the laminar variations in BOLD activity. Second, they allowed the averaging of fMRI data with depth in tissue. This averaging technique further improved the SNR. Moreover, when required data could be averaged over depth ranges that correspond to specific laminae within the tissue. Finally, they enabled the visualization of data on 3D representations of the SC.

In this dissertation, I confirm the retinotopic organization of the visual field in humans, and show that it is very similar to the long known organization in non-human primates (Cynader and Berman, 1972; Goldberg and Wurtz, 1972a; Schiller and Stryker, 1972). Recent fMRI work had also shown such a retinotopic representation along the polar angle dimension (Schneider and Kastner, 2005, 2009). I extend this by showing full maps for both polar angle and eccentricity and at a finer spatial scale. From the data presented here it seems that the previous inability to measure retinotopic organization along eccentricity may have had to do with multiple factors, among them, the stimulus FOV, spatial sampling and possible asymmetry in blood perfusion along the rostral-caudal axis on the SC surface. In general, the maps of eccentricity had a weaker SNR than polar angle with a statistically reliable progression observed in only a third of the

measured colliculi as compared to over three-fourth of the measured colliculi for polar angle. However, the sample size of the SCs under study was lesser for eccentricity compared to polar angle. Upon visual inspection, however, the proportion of colliculi out of the total measured, in which the direction of retinotopy could be observed along the direction expected from monkey maps was about similar between eccentricity and polar angle. The eccentricity stimulation data in Fig. 11 shows that signal quality was best in the rostral most region of the SC, worse near the middle and tended to recover toward the caudal portions. This suggests that the challenge in measuring eccentricity maps may have to do with the difficulty in deploying attention to gradually changing eccentricities compared to iso-eccentric polar angle shifts. Alternatively, there may be blood perfusion asymmetries across SC surface. Blood perfusion experiments would be required out to test the hypothesis of BOLD response asymmetries causing variations in data quality across SC. Such perfusion experiments can be carried out using a simple breath holding versus normal breathing paradigm (Kastrup et al., 1998; Li et al., 1999; Liu et al., 2002).

The representation of attention also seems to roughly follow a retinotopic organization and shows spatial registration with visual stimulation signals in SC. This is consistent with findings in monkeys where attentional modulation effects of attention are known to be spatially specific (Cavanaugh and Wurtz, 2004; Ignashchenkova et al., 2004; Muller et al., 2005; Wurtz and Mohler, 1976). Even though, for eccentricity measurements there was some amount of spatial misalignment (~1.7 mm offset) between visual stimulation and attention, the spatial topography of attention signals often followed the direction of the retinotopy.

In general, SNR was weaker for attention as compared to visual stimulation sessions. For datasets where the coherence fits were of low quality (coherence values < 0.20), multiple (2—3) sessions were averaged together. This multi-session averaging

substantially improved the data quality. All in all, ~80% of the attention datasets and ~20% of the visual stimulation datasets were averaged over multiple sessions. Another interesting observation was that often times the data on one side of the SC would be stronger and of better quality than the other side. Across subjects there was no consistent trend with regards to the left or right SC being better, which might have indicated handedness, since SC does have reach related signals (Linzenbold and Himmelbach, 2012). However, there was a general repeatability across sessions for each subject's "good" colliculus and "bad" colliculus, suggesting again the possibility of vascular noise artifacts or blood perfusion differences between each person's individual colliculi. Again, a blood perfusion experiments would help to test this hypothesis.

Once the retinotopic organization of visual stimulation and attention signals in SC has been established and it is known that these measurements can be made within a spatial precision of the order of millimeters (as compared to centimeters in cortex), carefully designed vision science experiments can be carried out within independently defined retinotopic ROIs in the SC. One such experiment was performed and formed the final part of this dissertation, Chapter V. Moreover, the retinotopic mapping techniques developed here would also be useful in the application of these methods to clinical populations, as discussed below.

It has been known that within early visual cortex, in addition to attention enhancing the fMRI BOLD response of visual stimuli, there is also a spatially specific boost in BOLD response for sustained endogenous attention in the absence of a visual stimulus, an attentional "base response" (Kastner et al., 1999; Ress et al., 2000; Silver et al., 2007). The presence of such a base response was demonstrated in the human SC. In the past there has been some disagreement in monkey literature as to whether the role of attention in SC is exogenous or endogenous (Cavanaugh and Wurtz, 2004;

Ignashchenkova et al., 2004; Muller et al., 2005). By counter-balancing the minimal bottom up drive using a threshold-contrast detection paradigm it is shown here that there is an endogenous modulation of attention within SC at least in humans. Furthermore, base response was compared with the conventional attention response to high-contrast visual stimulation in terms of their depth profiles within SC. It was found that fMRI base response peaked more deeply into the SC tissue than the response for attention to stimulation. This result is proposed to reflect the specific attentional enhancement of the intermediate layers after reduction in the visual drive of the superficial layers, which are known to have an attentional boost only with an accompanying visual stimulus. Such a proposal is in agreement with the oculomotor theory of attention and the role of SC in mediating covert attention. Moreover, if such a dissociation of attention into two components, visual vs. visuomotor (Ignashchenkova et al., 2004), is correct, then it generates new hypotheses for studying the role of other subcortical regions in attention to which SC is connected, such as pulvinar and LGN. From published monkey experiments, it is known that the pulvinar nucleus has multiple visual subdivisions, among them dorsomedial (Pdm) and inferior pulvinar (Pi). Of these, Pdm is the one known to be modulated by attention, while Pi, which is known to get projections from superficial layer visual neurons of SC, is not modulated by attention (Berman and Wurtz, 2011; Grieve et al., 2000; Robinson and Petersen, 1992). Human fMRI experiments, however, have shown attentional modulation in areas that are homologous to both Pdm and Pi (Kastner et al., 2004; Smith et al., 2009). Reasons for these differences are unclear. Based on the findings presented here and a possible visual versus visuomotor dichotomy of mechanisms of attention in SC, one hypothesis to study could be that SC sends out only the intermediate layer visuomotor attention signals. This would also be in agreement with the oculomotor theory of attention and would be similar to another role SC is known to

play, viz., sending out efferent copies of saccadic eye movement signals (Sommer and Wurtz, 2002, 2004). Performing high-resolution fMRI experiments that examine thalamic nuclei such as the pulvinar using a paradigm similar to the base response paradigm used here may help elucidate a possible visual versus visuomotor attentional distinction.

From a clinical standpoint SC has been implicated in the phenomenon of blindsight, which is the residual visual function after complete or partial cortical blindness (scotomas) (Cowey and Stoerig, 1991; Stoerig and Cowey, 1997). SC gets direct projections from the retina, and projects to cortical areas independent of the mainstream retino-geniculate to V1 pathway. Patients with blindsight report no conscious visual experience in certain parts of the visual field (or the entire visual field, though such cases are rare) but can still perform well above chance at tasks such as spatial localization and motion discrimination of objects within their scotoma. To date, there are no known studies of the role played by SC in blindsight using functional imaging techniques. The retinotopic mapping procedures presented in this work would provide a platform in being able to initiate such studies. A simple first experiment would be to investigate whether or not there is a retinotopic response for a visual stimulus in the blind field of such patients. If such a response is found, then stimuli of different features could be used to test what kind stimulus feature space is best conveyed through this subcortical pathway. These experiments may have great potential for finding better therapeutic and interventional techniques for the rehabilitation of cortically blind patients.

Bibliography

Anderson, E.J., and Rees, G. (2011). Neural correlates of spatial orienting in the human superior colliculus. Journal of neurophysiology 106, 2273-2284.

Awh, E., and Pashler, H. (2000). Evidence for split attentional foci. Journal of Experimental Psychology Human Perception and Performance 26, 834-846.

Beauchamp, M.S., Petit, L., Ellmore, T.M., Ingeholm, J., and Haxby, J.V. (2001). A parametric fMRI study of overt and covert shifts of visuospatial attention. Neuroimage 14, 310-321.

Bell, A.H., Fecteau, J.H., and Munoz, D.P. (2004). Using auditory and visual stimuli to investigate the behavioral and neuronal consequences of reflexive covert orienting. Journal of neurophysiology 91, 2172-2184.

Benevento, L.A., and Standage, G.P. (1983). The organization of projections of the retinorecipient and nonretinorecipient nuclei of the pretectal complex and layers of the superior colliculus to the lateral pulvinar and medial pulvinar in the macaque monkey. Journal of Comparative Neurology 217, 307-336.

Berman, R.A., and Wurtz, R.H. (2011). Signals conveyed in the pulvinar pathway from superior colliculus to cortical area MT. J Neurosci 31, 373-384.

Biswal, B., Zerrin Yetkin, F., Haughton, V.M., and Hyde, J.S. (1995). Functional connectivity in the motor cortex of resting human brain using echo,Äêplanar mri. Magnetic Resonance in Medicine 34, 537-541.

Brainard, D.H. (1997). The Psychophysics Toolbox. Spat Vis 10, 433-436.

Brefczynski, J.A., and DeYoe, E.A. (1999). A physiological correlate of the 'spotlight' of visual attention. Nat Neurosci 2, 370-374.

Brefczynski-Lewis, J.A., Datta, R., Lewis, J.W., and DeYoe, E.A. (2009). The topography of visuospatial attention as revealed by a novel visual field mapping technique. Journal of Cognitive Neuroscience 21, 1447-1460.

Buchel, C., Josephs, O., Rees, G., Turner, R., Frith, C.D., and Friston, K.J. (1998). The functional anatomy of attention to visual motion. A functional MRI study. Brain 121, 1281-1294.

Cavanaugh, J., Alvarez, B.D., and Wurtz, R.H. (2006). Enhanced performance with brain stimulation: attentional shift or visual cue? J Neurosci 26, 11347-11358.

Cavanaugh, J., and Wurtz, R.H. (2004). Subcortical modulation of attention counters change blindness. J Neurosci 24, 11236-11243.

Cohen, M.R., and Maunsell, J.H. (2009). Attention improves performance primarily by reducing interneuronal correlations. Nat Neurosci 12, 1594-1600.

Corbetta, M. (1998). Frontoparietal cortical networks for directing attention and the eye to visual locations: identical, independent, or overlapping neural systems? Proc Natl Acad Sci U S A 95, 831-838.

Corbetta, M., Akbudak, E., Conturo, T.E., Snyder, A.Z., Ollinger, J.M., Drury, H.A., Linenweber, M.R., Petersen, S.E., Raichle, M.E., and Van Essen, D.C. (1998). A common network of functional areas for attention and eye movements. Neuron 21, 761-773.
Corbetta, M., and Shulman, G.L. (2002). Control of goal-directed and stimulus-driven attention in the brain. Nature reviews neuroscience 3, 215-229.
Cowey, A., and Stoerig, P. (1991). The neurobiology of blindsight. Trends in neurosciences 14, 140-145.
Cynader, M., and Berman, N. (1972). Receptive-field organization of monkey superior colliculus. J Neurophysiol 35, 187-201.
de Haan, B., Morgan, P.S., and Rorden, C. (2008). Covert orienting of attention and overt eye movements activate identical brain regions. Brain research 1204, 102.
DeYoe, E.A., Bandettini, P., Neitz, J., Miller, D., and Winans, P. (1994). Functional magnetic resonance imaging (FMRI) of the human brain. Journal of neuroscience methods 54, 171-187.
DeYoe, E.A., Carman, G.J., Bandettini, P., Glickman, S., Wieser, J., Cox, R., Miller, D., and Neitz, J. (1996). Mapping striate and extrastriate visual areas in human cerebral cortex. Proc Natl Acad Sci U S A 93, 2382-2386.
Drager, U., and Hubel, D.H. (1975). Responses to visual stimulation and relationship between visual, auditory, and somatosensory inputs in mouse superior colliculus. Journal of neurophysiology 38, 690-713.
DuBois, R., and Cohen, M. (2000). Spatiotopic organization in human superior colliculus observed with fMRI. Neuroimage 12, 63-70.
Edwards, S.B., Ginsburgh, C.L., Henkel, C.K., and Stein, B.E. (1979). Sources of subcortical projections to the superior colliculus in the cat. Journal of Comparative Neurology 184, 309-329.
Engel, S.A., Glover, G.H., and Wandell, B.A. (1997). Retinotopic organization in human visual cortex and the spatial precision of functional MRI. Cereb Cortex 7, 181-192.
Fecteau, J.H., Bell, A.H., and Munoz, D.P. (2004). Neural correlates of the automatic and goal-driven biases in orienting spatial attention. Journal of neurophysiology 92, 1728-1737.
Ferrier, D. (1890). The Croonian lectures on cerebral localisation. British medical journal 2, 68.
Finlay, B.L., Schneps, S.E., Wilson, K.G., and Schneider, G.E. (1978). Topography of visual and somatosensory projections to the superior colliculus of the golden hamster. Brain research 142, 223-235.
Freedman, E.G., and Sparks, D.L. (1997). Activity of cells in the deeper layers of the superior colliculus of the rhesus monkey: evidence for a gaze displacement command. Journal of neurophysiology 78, 1669-1690.
Fries, W. (1984). Cortical projections to the superior colliculus in the macaque monkey: a retrograde study using horseradish peroxidase. Journal of Comparative Neurology 230, 55-76.

Fries, W., and Distel, H. (1983). Large layer VI neurons of monkey striate cortex (Meynert cells) project to the superior colliculus. Proceedings of the Royal Society of London Series B Biological Sciences 219, 53-59.
Friston, K., Josephs, O., Zarahn, E., Holmes, A., Rouquette, S., and Poline, J.-B. (2000). To smooth or not to smooth?: Bias and efficiency in fmri time-series analysis. Neuroimage 12, 196-208.
Garcia-Perez, M.A. (1998). Forced-choice staircases with fixed step sizes: asymptotic and small-sample properties. Vision Res 38, 1861-1881.
Gitelman, D.R., Parrish, T.B., Friston, K.J., and Mesulam, M.-M. (2002). Functional anatomy of visual search: regional segregations within the frontal eye fields and effective connectivity of the superior colliculus. Neuroimage 15, 970-982.
Glover, G.H. (1999). Simple analytic spiral K-space algorithm. Magn Reson Med 42, 412-415.
Glover, G.H., and Lai, S. (1998). Self-navigated spiral fMRI: interleaved versus single-shot. Magn Reson Med 39, 361-368.
Glover, G.H., Li, T.-Q., and Ress, D. (2000). Image,Äêbased method for retrospective correction of physiological motion effects in fMRI: RETROICOR. Magnetic Resonance in Medicine 44, 162-167.
Goldberg, M.E., and Wurtz, R.H. (1972a). Activity of superior colliculus in behaving monkey. I. Visual receptive fields of single neurons. J Neurophysiol 35, 542-559.
Goldberg, M.E., and Wurtz, R.H. (1972b). Activity of superior colliculus in behaving monkey. II. Effect of attention on neuronal responses. J Neurophysiol 35, 560-574.
Goldman, P.S., and Nauta, W.J. (1976). Autoradiographic demonstration of a projection from prefrontal association cortex to the superior colliculus in the rhesus monkey. Brain research 116, 145.
Grieve, K.L., Acuna, C., and Cudeiro, J. (2000). The primate pulvinar nuclei: vision and action. Trends in neurosciences 23, 35-39.
Groh, J.M., and Sparks, D.L. (1996). Saccades to somatosensory targets. III. Eye-position-dependent somatosensory activity in primate superior colliculus. Journal of neurophysiology 75, 439-453.
Harel, N., Lin, J., Moeller, S., Ugurbil, K., and Yacoub, E. (2006). Combined imaging-histological study of cortical laminar specificity of fMRI signals. Neuroimage 29, 879-887.
Harting, J.K., Huerta, M.F., Frankfurter, A.J., Strominger, N.L., and Royce, G.J. (1980). Ascending pathways from the monkey superior colliculus: an autoradiographic analysis. Journal of Comparative Neurology 192, 853-882.
Harting, J.K., Updyke, B.V., and van Lieshout, D.P. (1992). Corticotectal projections in the cat: Anterograde transport studies of twenty,Äêfive cortical areas. Journal of Comparative Neurology 324, 379-414.
Haynes, J.-D., Deichmann, R., and Rees, G. (2005). Eye-specific effects of binocular rivalry in the human lateral geniculate nucleus. Nature 438, 496-499.
Hoffman, J.E., and Subramaniam, B. (1995). The role of visual attention in saccadic eye movements. Perception & Psychophysics 57, 787-795.

Holmes, A., Josephs, O., Buchel, C., and Friston, K. (1997). Statistical modelling of low-frequency confounds in fMRI. Neuroimage 5, S480.
Huk, A.C., Ress, D., and Heeger, D.J. (2001). Neuronal basis of the motion aftereffect reconsidered. Neuron 32, 161-172.
Ignashchenkova, A., Dicke, P.W., Haarmeier, T., and Thier, P. (2004). Neuron-specific contribution of the superior colliculus to overt and covert shifts of attention. Nat Neurosci 7, 56-64.
Jay, M.F., and Sparks, D.L. (1987). Sensorimotor integration in the primate superior colliculus. II. Coordinates of auditory signals. Journal of neurophysiology 57, 35-55.
Kastner, S., O'Connor, D.H., Fukui, M.M., Fehd, H.M., Herwig, U., and Pinsk, M.A. (2004). Functional imaging of the human lateral geniculate nucleus and pulvinar. J Neurophysiol 91, 438-448.
Kastner, S., and Pinsk, M.A. (2004). Visual attention as a multilevel selection process. Cognitive, Affective, & Behavioral Neuroscience 4, 483-500.
Kastner, S., Pinsk, M.A., De Weerd, P., Desimone, R., and Ungerleider, L.G. (1999). Increased activity in human visual cortex during directed attention in the absence of visual stimulation. Neuron 22, 751-761.
Kastner, S., and Ungerleider, L.G. (2000). Mechanisms of visual attention in the human cortex. Annu Rev Neurosci 23, 315-341.
Kastrup, A., Li, T.-Q., Takahashi, A., Glover, G.H., and Moseley, M.E. (1998). Functional magnetic resonance imaging of regional cerebral blood oxygenation changes during breath holding. Stroke 29, 2641-2645.
Katyal, S., Greene, C., and Ress, D. (2012). High-resolution Functional Magnetic Resonance Imaging Methods for Human Midbrain. J Vis Exp.
Katyal, S., Zughni, S., Greene, C., and Ress, D. (2010). Topography of covert visual attention in human superior colliculus. J Neurophysiol 104, 3074-3083.
Khan, R., Zhang, Q., Darayan, S., Dhandapani, S., Katyal, S., Greene, C., Bajaj, C., and Ress, D. (2011). Surface-based analysis methods for high-resolution functional magnetic resonance imaging. Graphical models 73, 313-322.
King, K.F., Ganin, A., Zhou, X.J., and Bernstein, M.A. (1999). Concomitant gradient field effects in spiral scans. Magn Reson Med 41, 103-112.
Klein, R. (1980). Does oculomotor readiness mediate cognitive control of visual attention. Attention and performance VIII 8, 259-276.
Komatsu, H., and Suzuki, H. (1985). Projections from the functional subdivisions of the frontal eye field to the superior colliculus in the monkey. Brain research 327, 324-327.
Kramer, A.F., and Hahn, S. (1995). Splitting the beam: Distribution of attention over noncontiguous regions of the visual field. Psychological Science, 381-386.
Krebs, R., Woldorff, M., Tempelmann, C., Bodammer, N., Noesselt, T., Boehler, C., Scheich, H., Hopf, J., Duzel, E., and Heinze, H. (2010). High-Field fMRI Reveals Brain Activation Patterns Underlying Saccade Execution in the Human Superior Colliculus. PLoS ONE 5, 8691.
Kruger, G., and Glover, G.H. (2001). Physiological noise in oxygenation-sensitive magnetic resonance imaging. Magnetic Resonance in Medicine 46, 631-637.

Kunzle, H., Akert, K., and Wurtz, R.H. (1976). Projection of area 8 (frontal eye field) to superior colliculus in the monkey. An autoradiographic study. Brain Res 117, 487-492.
Kustov, A.A., and Robinson, D.L. (1996). Shared neural control of attentional shifts and eye movements. Nature 384, 74-77.
Lee, C., Rohrer, W.H., and Sparks, D.L. (1988). Population coding of saccadic eye movements by neurons in the superior colliculus. Nature 332, 357-360.
Leventhal, A.G., Rodieck, R., and Dreher, B. (1981). Retinal ganglion cell classes in the Old World monkey: morphology and central projections. Science 213, 1139-1142.
Li, T.-Q., Kastrup, A., Takahashi, A.M., and Moseley, M.E. (1999). Functional MRI of human brain during breath holding by BOLD and FAIR techniques. Neuroimage 9, 243-249.
Linzenbold, W., and Himmelbach, M. (2012). Signals from the Deep: Reach-Related Activity in the Human Superior Colliculus. The Journal of neuroscience 32, 13881-13888.
Linzenbold, W., Lindig, T., and Himmelbach, M. (2011). Functional neuroimaging of the oculomotor brainstem network in humans. Neuroimage 57, 1116-1123.
Liu, H.-L., Huang, J.-C., Wu, C.-T., and Hsu, Y.-Y. (2002). Detectability of blood oxygenation level-dependent signal changes during short breath hold duration. Magnetic resonance imaging 20, 643-648.
Logothetis, N.K., Pauls, J., Augath, M., Trinath, T., and Oeltermann, A. (2001). Neurophysiological investigation of the basis of the fMRI signal. Nature 412, 150-157.
Logothetis, N.K., and Wandell, B.A. (2004). Interpreting the BOLD signal. Annu Rev Physiol 66, 735-769.
Lovejoy, L.P., and Krauzlis, R.J. (2009). Inactivation of primate superior colliculus impairs covert selection of signals for perceptual judgments. Nat Neurosci 13, 261-266.
Lu, H., Patel, S., Luo, F., Li, S.J., Hillard, C.J., Ward, B.D., and Hyde, J.S. (2004). Spatial correlations of laminar BOLD and CBV responses to rat whisker stimulation with neuronal activity localized by Fos expression. Magn Reson Med 52, 1060-1068.
Luck, S.J., Chelazzi, L., Hillyard, S.A., and Desimone, R. (1997). Neural mechanisms of spatial selective attention in areas V1, V2, and V4 of macaque visual cortex. J Neurophysiol 77, 24-42.
Lui, F., Gregory, K.M., Blanks, R.H., and Giolli, R.A. (1995). Projections from visual areas of the cerebral cortex to pretectal nuclear complex, terminal accessory optic nuclei, and superior colliculus in macaque monkey. Journal of Comparative Neurology 363, 439-460.
Lynch, J., Graybiel, A., and Lobeck, L. (1985). The differential projection of two cytoarchitectonic subregions of the inferior parietal lobule of macaque upon the deep layers of the superior colliculus. Journal of Comparative Neurology 235, 241-254.
Marrocco, R., and Li, R. (1977). Monkey superior colliculus: properties of single cells and their afferent inputs. Journal of neurophysiology 40, 844-860.
Maunsell, J.H., and Treue, S. (2006). Feature-based attention in visual cortex. Trends in neurosciences 29, 317-322.

May, P.J. (2006). The mammalian superior colliculus: laminar structure and connections. Progress in brain research 151, 321.
Mays, L.E., and Sparks, D.L. (1980). Dissociation of visual and saccade-related responses in superior colliculus neurons. Journal of neurophysiology 43, 207-232.
McAlonan, K., Cavanaugh, J., and Wurtz, R.H. (2008). Guarding the gateway to cortex with attention in visual thalamus. Nature 456, 391-394.
McMains, S.A., and Somers, D.C. (2004). Multiple spotlights of attentional selection in human visual cortex. Neuron 42, 677-686.
Meredith, M., Wallace, M., and Stein, B. (1992). Visual, auditory and somatosensory convergence in output neurons of the cat superior colliculus: multisensory properties of the tecto-reticulo-spinal projection. Experimental Brain Research 88, 181-186.
Meredith, M.A., Clemo, H.R., and Stein, B.E. (1991). Somatotopic component of the multisensory map in the deep laminae of the cat superior colliculus. Journal of Comparative Neurology 312, 353-370.
Mitchell, J.F., Sundberg, K.A., and Reynolds, J.H. (2007). Differential attention-dependent response modulation across cell classes in macaque visual area V4. Neuron 55, 131-141.
Mooney, R.D., Nikoletseas, M.M., Hess, P.R., Allen, Z., Lewin, A.C., and Rhoades, R.W. (1988). The projection from the superficial to the deep layers of the superior colliculus: an intracellular horseradish peroxidase injection study in the hamster. The Journal of neuroscience 8, 1384-1399.
Moore, T., and Armstrong, K.M. (2003). Selective gating of visual signals by microstimulation of frontal cortex. Nature 421, 370-373.
Moore, T., Armstrong, K.M., and Fallah, M. (2003). Visuomotor origins of covert spatial attention. Neuron 40, 671-683.
Moore, T., and Fallah, M. (2004). Microstimulation of the frontal eye field and its effects on covert spatial attention. J Neurophysiol 91, 152-162.
Moschovakis, A., Karabelas, A., and Highstein, S. (1988). Structure-function relationships in the primate superior colliculus. I. Morphological classification of efferent neurons. Journal of neurophysiology 60, 232-262.
Muller, J.R., Philiastides, M.G., and Newsome, W.T. (2005). Microstimulation of the superior colliculus focuses attention without moving the eyes. Proc Natl Acad Sci USA 102, 524-529.
Munoz, D., and Wurtz, R. (1993). Fixation cells in monkey superior colliculus. II. Reversible activation and deactivation. J Neurophysiol 70, 576.
Munoz, D.P., and Wurtz, R.H. (1995a). Saccade-related activity in monkey superior colliculus. I. Characteristics of burst and buildup cells. J Neurophysiol 73, 2313-2333.
Munoz, D.P., and Wurtz, R.H. (1995b). Saccade-related activity in monkey superior colliculus. II. Spread of activity during saccades. Journal of neurophysiology 73, 2334-2348.
Nestares, O., and Heeger, D.J. (2000). Robust multiresolution alignment of MRI brain volumes. Magn Reson Med 43, 705-715.

Nobre, A., Gitelman, D., Dias, E., and Mesulam, M. (2000). Covert visual spatial orienting and saccades: overlapping neural systems. Neuroimage 11, 210-216.
O'Connor, D.H., Fukui, M.M., Pinsk, M.A., and Kastner, S. (2002). Attention modulates responses in the human lateral geniculate nucleus. Nat Neurosci 5, 1203-1209.
Paxinos, G., and Mai, J.K. (2004). The Human Nervous System, Second edn (New York: Academic Press).
Pelli, D.G. (1997). The VideoToolbox software for visual psychophysics: Transforming numbers into movies. Spatial vision 10, 437-442.
Perry, R., and Zeki, S. (2000). The neurology of saccades and covert shifts in spatial attention An event-related fMRI study. Brain 123, 2273-2288.
Perry, V., and Cowey, A. (1984). Retinal ganglion cells that project to the superior colliculus and pretectum in the macaque monkey. Neuroscience 12, 1125-1137.
Petit, L., and Beauchamp, M.S. (2003). Neural basis of visually guided head movements studied with fMRI. Journal of neurophysiology 89, 2516-2527.
Pfeuffer, J., de Moortele, V., Ugurbil, K., Hu, X., and Glover, G.H. (2002). Correction of physiologically induced global off,Äêresonance effects in dynamic echo,Äêplanar and spiral functional imaging. Magnetic Resonance in Medicine 47, 344-353.
Pollack, J., and Hickey, T. (1979). The distribution of retino-collicular axon terminals in rhesus monkey. Journal of Comparative Neurology 185, 587-602.
Posner, M.I. (1980). Orienting of attention. Q J Exp Psychol 32, 3-25.
Posner, M.I., and Petersen, S.E. (1989). The attention system of the human brain. (DTIC Document).
Posner, M.I., Rafal, R.D., Choate, L.S., and Vaughan, J. (1985). Inhibition of return: Neural basis and function. Cognitive Neuropsychology 2, 211-228.
Rafal, R.D. (1994). Neglect. Current opinion in neurobiology 4, 231-236.
Rafal, R.D., Posner, M.I., Friedman, J.H., Inhoff, A.W., and Bernstein, E. (1988). Orienting of visual attention in progressive supranuclear palsy. Brain 111, 267-280.
Ress, D., Backus, B.T., and Heeger, D.J. (2000). Activity in primary visual cortex predicts performance in a visual detection task. Nat Neurosci 3, 940-945.
Ress, D., Glover, G.H., Liu, J., and Wandell, B. (2007). Laminar profiles of functional activity in the human brain. Neuroimage 34, 74-84.
Reynolds, J.H., and Chelazzi, L. (2004). Attentional modulation of visual processing. Annu Rev Neurosci 27, 611-647.
Rizzolatti, G., Riggio, L., Dascola, I., and Umilta, C. (1987). Reorienting attention across the horizontal and vertical meridians: evidence in favor of a premotor theory of attention. Neuropsychologia 25, 31-40.
Rizzolatti, G., Riggio, L., and Sheliga, B.M. (1994). Space and Selective Attention. In Attention and performance XV: conscious and nonconscious information processing, C. Umiltà, and M. Moscovitch, eds. (Massachusetts: The MIT Press), pp. 231-264.
Robinson, D.A. (1972). Eye movements evoked by collicular stimulation in the alert monkey. Vision Res 12, 1795-1808.
Robinson, D.L., and Petersen, S.E. (1992). The pulvinar and visual salience. Trends in neurosciences 15, 127-132.

Sapir, A., Soroker, N., Berger, A., and Henik, A. (1999). Inhibition of return in spatial attention: direct evidence for collicular generation. Nat Neurosci 2, 1053-1054.
Schiller, P., and Stryker, M. (1972). Single-unit recording and stimulation in superior colliculus of the alert rhesus monkey. J Neurophysiol 35, 915.
Schiller, P.H., and Koerner, F. (1971). Discharge characteristics of single units in superior colliculus of the alert rhesus monkey. J neurophysiol 34, 920-935.
Schneider, K.A., and Kastner, S. (2005). Visual responses of the human superior colliculus: a high-resolution functional magnetic resonance imaging study. J Neurophysiol 94, 2491-2503.
Schneider, K.A., and Kastner, S. (2009). Effects of sustained spatial attention in the human lateral geniculate nucleus and superior colliculus. J Neurosci 29, 1784-1795.
Sereno, M.I., Dale, A.M., Reppas, J.B., Kwong, K.K., Belliveau, J.W., Brady, T.J., Rosen, B.R., and Tootell, R.B. (1995). Borders of multiple visual areas in humans revealed by functional magnetic resonance imaging. Science 268, 889-893.
Shepherd, M., Findlay, J.M., and Hockey, R.J. (1986). The relationship between eye-movements and spatial attention. Q J Exp Psychol Sect A-Hum Exp Psychol 38, 475-491.
Silver, M., Ress, D., and Heeger, D. (2005). Topographic maps of visual spatial attention in human parietal cortex. J Neurophysiol 94, 1358.
Silver, M.A., Ress, D., and Heeger, D.J. (2007). Neural correlates of sustained spatial attention in human early visual cortex. J Neurophysiol 97, 229-237.
Smith, A.T., Cotton, P.L., Bruno, A., and Moutsiana, C. (2009). Dissociating vision and visual attention in the human pulvinar. J Neurophysiol 101, 917-925.
Sommer, M.A., and Wurtz, R.H. (2000). Composition and topographic organization of signals sent from the frontal eye field to the superior colliculus. J Neurophysiol 83, 1979-2001.
Sommer, M.A., and Wurtz, R.H. (2002). A pathway in primate brain for internal monitoring of movements. Science 296, 1480-1482.
Sommer, M.A., and Wurtz, R.H. (2004). What the brain stem tells the frontal cortex. I. Oculomotor signals sent from superior colliculus to frontal eye field via mediodorsal thalamus. J Neurophysiol 91, 1381-1402.
Sparks, D.L., and Hartswich-Young, R. (1989). The deep layers of the superior colliculus. In The Neurobiology of Saccadic Eye Movements, R.H. Wurtz, and M.E. Goldberg, eds. (Elsevier Science Publishers), pp. 213-255.
Sparks, D.L., Holland, R., and Guthrie, B.L. (1976). Size and distribution of movement fields in the monkey superior colliculus. Brain research 113, 21-34.
Sparks, D.L., and Nelson, I.S. (1987). Sensory and motor maps in the mammalian superior colliculus. Trends in neurosciences 10, 312-317.
Sprague, J.M. (1966). Interaction of cortex and superior colliculus in mediation of visually guided behavior in the cat. Science 153, 1544-1547.
Stein, B.E., Wallace, M.T., and Stanford, T.R. (2002). Superior colliculus. In Encyclopedia of the human brain, V. Ramachandran, ed. (Amsterdam: Elsevier), pp. 503-520.
Stoerig, P., and Cowey, A. (1997). Blindsight in man and monkey. Brain 120, 535-559.

Tardif, E., and Clarke, S. (2002). Commissural connections of human superior colliculus. Neuroscience 111, 363-372.
Tiao, Y.C., and Blakemore, C. (1976). Functional organization in the superior colliculus of the golden hamster. J Comp Neurol 168, 483-503.
von Helmholtz, H. (1866/1962). Helmholtz's treatise on physiological optics. Vol. 2: The sensation of vision, trans. JPC Southall. (Translated from the third German edition). (Dover.[VV]).
Wall, M., Walker, R., and Smith, A. (2009). Functional imaging of the human superior colliculus: an optimised approach. Neuroimage 47, 1620-1627.
Wallace, M.T., Meredith, M.A., and Stein, B.E. (1993). Converging influences from visual, auditory, and somatosensory cortices onto output neurons of the superior colliculus. Journal of neurophysiology 69, 1797-1809.
Wallace, M.T., Wilkinson, L.K., and Stein, B.E. (1996). Representation and integration of multiple sensory inputs in primate superior colliculus. J Neurophysiol 76, 1246-1266.
Walton, M.M., Bechara, B., and Gandhi, N.J. (2007). Role of the primate superior colliculus in the control of head movements. Journal of neurophysiology 98, 2022-2037.
Wandell, B.A., Chial, S., and Backus, B.T. (2000). Visualization and measurement of the cortical surface. Journal of Cognitive Neuroscience 12, 739-752.
Weddell, R.A. (2004). Subcortical modulation of spatial attention including evidence that the Sprague effect extends to man. Brain and cognition 55, 497-506.
Wilson, J.R., Hendrickson, A.E., Sherk, H., and Tigges, J. (1995). Sources of subcortical afferents to the macaque's dorsal lateral geniculate nucleus. The Anatomical Record 242, 566-574.
Worsley, K.J., and Friston, K.J. (1995). Analysis of fMRI time-series revisited, Again. Neuroimage 2, 173-181.
Wurtz, R.H., and Albano, J.E. (1980). Visual-motor function of the primate superior colliculus. Annual review of neuroscience 3, 189-226.
Wurtz, R.H., and Goldberg, M.E. (1972). Activity of superior colliculus in behaving monkey. III. Cells discharging before eye movements. J Neurophysiol 35, 575-586.
Wurtz, R.H., and Mohler, C.W. (1976). Organization of monkey superior colliculus: enhanced visual response of superficial layer cells. J Neurophysiol 39, 745-765.
Xu, G., Pan, Q., and Bajaj, C.L. (2006). Discrete Surface Modeling Using Partial Differential Equations. Computer Aided Geometric Design 23, 125-145.
Yushkevich, P.A., Piven, J., Hazlett, H.C., Smith, R.G., Ho, S., Gee, J.C., and Gerig, G. (2006). User-guided 3D active contour segmentation of anatomical structures: significantly improved efficiency and reliability. Neuroimage 31, 1116-1128.
Zenon, A., and Krauzlis, R.J. (2012). Attention deficits without cortical neuronal deficits. Nature.